Distribution of Adhesive in Particle Boards

Master Thesis

Submitted by

Clemens Josef Schmidberger

Supervisor: Univ. Prof. Dr. Wolfgang Gindl-Altmutter

Co-supervisor: Eike Mahrdt, MSc.

Institute of Wood Science and Technology

Department of Material Sciences and Process Engineering

University of Natural Resources and Applied Life Sciences

BOKU – Vienna

April 2015

Acknowledgement

One of my favorite German musicians has once sang in a song: “*Du hast mir die Hälfte erzählt von allem was ich weiß: die schlausten Dinge, die besten Geschichten, die traurigsten Dramen und den größten Schei**.*” (Tomte, 2008) I think this song text is a simplified but pretty accurate summary of and tribute to my academic studies in the last seven years. Because university is not just about gaining knowledge, studying, exams and grades, in German summarized under the term *Ausbildung*. But it is also about gaining life experience, celebrating, culture, enjoying holidays, traveling and so on. If we combine all of that and consider the fact that my studies are *Aus* (over) and eliminate this term from the term ~~Aus~~bildung, we get the term *Bildung.* And this is what I can look back on, and this is why I am so thankful to all those people who made the last seven years possible. Special thanks to my family: my parents Johanna and Reinhard, my grandparents Maria and Josef and my siblings. Many thanks to all my friends who spent the last years with me and made it such a great time. Special thanks go to my friends, fellow students and flatmates Eva and David who supported me in tough study times and with whom I spent a lot of evenings of *Holz* - discussions and had a lot of fun. Last but not least many thanks to Prof. Wolfgang Gindl-Altmutter and Eike Mahrdt MSc. for supervising this master thesis.

Abstract

The internal bond strength test of particle board samples with UF-adhesive reinforced with nanocellulose or additive II showed significantly better results than the unreinforced reference samples. The hypothesis was that due to the additives the penetration of adhesive in the wood matter is reduced and thus more adhesive is available in the glue joint. This was proved with the novel method of adhesive detection, which determines the location of adhesive in particle boards. Therefore the adhesive was differentiated in three portions: adhesive in the glue joint, penetrating adhesive and excess adhesive. Specimens of a size of 3 x 4 x 3 mm were cut out of particle board bending samples. These samples were used to create thin slices, which were stained with the fluorescent-stain Brilliant Sulphaflavine and Genitanaviolet afterwards. The microscope images were edited with Photoshop in a way that the different portions could be calculated with binary operations. The hypothesis could not be proved, but the results show that the addition of additives results in more adhesive in the glue joint and significantly less excess. It could also be proved that the adhesive particle size distribution is dependent on the adhesive system. The reference samples show a tendency to a higher amount of smaller adhesive particles.

Keywords: adhesive, urea-formaldehyde, nanocellulose, detection, particle board, additive

Zusammenfassung

Die Querzugsfestigkeitsprüfung von Spanplattenproben mit einem Harnstoffformaldehydharz-Bindemittel verstärkt durch Nanozellulose oder Additiv 2, zeigten signifikant bessere Ergebnisse als die unverstärkten Referenzproben. Die Hypothese war, dass Additive die Penetration des Bindemittels in das Holzgefüge reduzieren und somit mehr Bindemittel in der Klebefuge für die Verklebung bleibt. Diese Annahme wurde mit der neuen Methode der Bindemittel Detektion überprüft. Dafür wurde das Bindemittel in drei verschiedene Anteile eingeteilt: Bindemittel in der Klebefuge, penetriertes Bindemittel und Überschuss. Proben mit einer Größe von 3 x 4 x 3 mm wurden aus Biegeproben herausgeschnitten. Daraus wurden in weiterer Folge Dünnschnitte hergestellt und mit dem Fluoreszenzmittel Brilliant Sulphaflavin und dem Färbemittel Gentianaviolett eingefärbt. Die Mikroskopbilder wurden mit

Photoshop so bearbeitet, dass anschließend über eine binäre Berechnungsmethode die jeweiligen Anteile bestimmt werden konnten. Die Hypothese konnte nicht bestätigt werden. Die Ergebnisse zeigten jedoch, dass die Beimengung der Additive zu mehr Bindemittel in der Klebefuge und signifikant weniger Überschuss führte. Weiters konnte herausgefunden werden, dass die Verteilung der Bindemittelpartikel-Größe vom Bindemittelsystem abhängig ist. Die Referenzproben zeigten eine Tendenz zu einer größeren Menge an kleinen Bindemittel-Partikeln.

Keywords: Bindemittel, Harnstoff-Formaldehyd, Nanozellulose, Detektion, Spanplatte, Additive

Table of Contents

1 Introduction

The particle board is by far the most used wood based panel in Europe and accounted for more than half (54%) of the overall wood based panel production in the year 2012 (UNECE and FAO 2013). Physical and mechanical properties of particle boards largely depend on the density of the wood based panel. Mechanical properties of wood based panels show a positive correlation between density and strength. This is due to the higher compression ratio of the particles and subsequently a higher contact area between the particles surface (Thoemen et al. 2010).

Increasing competition and price for the raw material, due to e.g. the bio energy action plan of the EU, increasing transportation costs due to higher oil prices and longer transport distances as a consequence of globalization, makes the particle boards producers want to shift to lighter particle boards and less wood raw material input. This can only be achieved by increasing the performance of the wood adhesive joints.

Adhesives for the particle board production are most commonly based on urea-formaldehyde followed by melamine-formaldehyde and belong to the category of the aminoplastic-adhesives (Dunky 1998; Habenicht 2008; Thoemen et al. 2010). The reasons for the high utilization of urea-formaldehyde resin are its low price, a clear or white glueline after curing, that it provides a good dry strength and that a lot of experience has been gathered in production with this adhesive system (Dunky 1998; Thoemen et al. 2010). But there are also some disadvantages such as the absence of hydrolyse resistance, the subsequent formaldehyde emissions and the relatively high stiffness of UF-resins compared to others (Dunky 1998; Müller et al. 2005). Müller et al. (2005) found out that due to the higher stiffness of aminoplastic resins compared to e.g. PUR, stress concentrations can occur in the glueline which decrease the overall strength of the adhesive. Urea-formaldehyde resin is also a highly brittle material and tends to create micro-cracks, which as a result also lower the mechanical performance. The high utilization in the wood based panel industry and the performance limiting factors, especially brittleness and a tendency to micro-cracks, makes urea-formaldehyde resins the best material to put focus on concerning improvement with different fillers (Eichhorn et al. 2010).

As the glue application for the major wood based panels (particle board, OSB) usually happens via spraying nozzles in which the resin is atomized in small droplets with a size from 30-100 μm, the size of the filler particles must be even smaller (Thoemen et al. 2010). Hence, cellulose nanofibers seem to be the most promising filler for the reinforcement of urea-formaldehyde resins. Cellulose nanofibers are mostly obtained from cellulose, which is the most abundant polymer on earth. Due to its high availability and the high cellulose amount wood is containing, it is preferably used as raw material. Besides, also other cellulose containing plants can act as a raw material e.g. flax, hemp, jute, ramie and cotton. But there are also existing non-plant sources of cellulose such as bacteria or tunicates. As we are focusing on cellulose nanofibers manufactured out of wood in this master thesis, the term nanofibers subsequently refers to nanofibers made out of wood. Cellulose nanofibers are in general produced by deconstructing the hierarchical structure of cellulose to a nano-scale. This breakdown into individualized nanofibers reduces the amount of amorphous material and generates nanofibers with a high crystallinity and hence, a higher strength and stiffness. Furthermore, the aspect-ratio (length/diameter) is increased by decreasing the fibrous structure of wood fibers. This high aspect ratio is especially important for achieving a good stress transfer from the matrix to the reinforced phase. Two main methods are used in the manufacturing of nanofibers from cellulosic plant material. The first method is to expose plant fibers to strong acidic conditions combined with sonication. The results of this method are so called nanowhiskers with a length between 100 and 300 nm. The second process resigns the use of chemical treatment, but uses high mechanical shearing forces for the disintegration of the fibers, and therefore generates a material called microfibrillated cellulose (Eichhorn et al. 2010).

Several researchers have investigated the suitability of nanofibers as a filler for reinforcing adhesives in the wood industry. Lopez-Suevos et al. (2010) for example reinforced poly vinyl acetate (PVAc) latex adhesive with different nanofibers for improving the heat resistance. On the other hand a lot of research has been conducted at the Institute of Wood Science and Technology in Vienna to improve the strength of urea-formaldehyde resins. Eichhorn et al. (2010) investigated the ability of cellulose nanofibers to reinforce a urea-formaldehyde adhesive when loaded with shear stress. For this experiment they used a water suspension with 5% cellulose of a dissolving grade beech pulp. The beech pulp was fibrillated by several homogenization processes and in the next step the suspension was vacuum-dried to a cellulose content of 3.2%. With this suspension a UF-adhesive mixture with 5% nanofibrils per unit weight cured resin was produced and tested on lap-joint shear test specimens according to EN 302 (2004). Also samples with unmodified UF-resin and UF-resin with 5 % un-homogenized beech pulp were tested. The results were surprising. There was no significant difference in shear strength of the adhesive with the untreated beech pulp compared to the reference, and both were within the same range of other wood adhesives shear strengths. On the other hand the adhesive with 5% cellulose nanofibrils outperformed the other two groups and showed a significantly higher shear strength as well as higher deformation to failure. The authors assume that the UF-resin has been toughened by adding nanofibrils and attribute this to the absence of micro-cracks, which can be commonly seen in UF-bondlines. The fact that the addition of untreated beech pulp has no influence on the shear strength underlines the statement of Eichhorn et al. (2010) that the higher the disintegration rate, the more crystalline areas in the cellulose fibers are achieved, hence resulting in higher strength and stiffness. This promising result led to further research carried out by Veigel et al. (2011) who investigated the effect of nanofibrils as filler in urea-formaldehyde adhesives on the specific fracture energy of solid-wood adhesives. Like in the previous experiment, they used a never dried dissolved grade beech pulp. Half of it was high pressure homogenized without pretreatment (P1) while the other half was chemically treated with a so called carboxylation to support the disintegration of the fiber bundles in the following high pressure homogenization (P2). Next to these two different manufactured nanofibrils, bacterial cellulose was also used as filler. Two different types of adhesives were used for the experiment, namely one non-structural powder adhesive for timber bonding and a low viscous urea-formaldehyde resin used for industrial particle board production. For each adhesive and filler mixtures with 0.5, 1, 1.5 and 2% of cellulose per unit weight UF were produced. It must be mentioned that there were some problems with adding the P2 cellulose to the UF-resin, because even after mixing small cellulose bundles could be observed. This may be reasoned on the difference in the structure of the nanofibrils as found out with FE-SEM microscopy. The bacterial and the untreated nanofibrils showed a loose network of cellulose fibrils after vacuum drying whereas the carboxylated fibrils built up a compact film after drying. The diameter of the nanofibrils was also measured and showed quite a difference with 61 ± 21 nm (P1), 96 ± 48 nm (P2) and 109 ± 56 nm (BC). Furthermore, the crystallinity was measured with WAXD and the highest crystallinity index c was 0.98 for BC, followed by 0.94 for P1 and 0.84 for P2. Investigations of the bondline showed one very interesting fact, namely that the addition of P1 to the particleboard adhesive considerably reduced the penetration of the resin in the wood, although the viscosity was only slightly higher than in the pure resin.

The mechanical fracture energy was tested with the simplified flat double cantilever beam specimen after Gagliano and Frazier (2001). There were several different effects observed on the specific fracture energy due to the addition of cellulose nanofibrils. First of all, it can be said that the variability of the modified specimen is higher compared to the unmodified. The authors see the reason for this in a potentially uneven distribution of the nanofibrils. For the specific fracture energy it can be said in general that improvement could be seen for both adhesives, but with UF-1 it was more often statistically significant than UF-2. If we take a closer look at the results of UF-1, it is obvious that the toughness is increasing with an increasing content of P1 cellulose. The highest improvement of 45% in specific fracture energy was achieved by adding 2% of nanofibrils to UF-1. The conclusion of this research is that it is possible to increase the specific fracture energy by using urea-formaldehyde resin that is reinforced either with unmodified cellulose nanofibrils or fibrillated bacterial cellulose. TEMPO-modified cellulose on the other hand did not show any significant improvement (Veigel et al. 2011).

As two studies (Eichhorn et al. 2010; Veigel et al. 2011) show a certain ability of cellulose nanofibrils to reinforce urea-formaldehyde resins when applied on solid wood, the next step would be to apply this innovation to wood-based panels, due to the much higher utilization of urea-formaldehyde based resins in the wood based panel industry. This is what Veigel et al. (2012) did in their next study, where they produced particle boards and oriented strand boards with nanocellulose reinforced adhesive and carried out several mechanical tests. Again never dried dissolving grade beech pulp was used for these experiments. The fibrillation process was carried out in a similar way as the two previous studies. For the characterization of the nanofibrils Atomic Force Microscopy (AFM) was used. The average diameter of the nanofibrils was much smaller (35 nm) as observed in the previous study (65 nm) (Veigel et al. 2011). A reason for this could be the increased number of passes through the high-pressure homogenizer. For the particle board production a UF-resin and for the OSB production a powdery MUF-resin, both are from the wood based panel industry, were used. For the particle boards resin suspensions with 1% and 3% nanofibrils were prepared and applied on the particles in a rotating drum mixer. Subsequently the glued particles were dried for various durations to remove excessive water. Not till then the hardener solution was sprayed on the particles. OSB boards with 1% nanofibrils were produced with the same glue application procedure. The resin content for particle boards was 10% and for OSB 8% of solid resin based on oven-dry wood. Summarizing the mechanical properties of the particle board, it can be said that there are no differences in the density but obvious differences were found in the thickness swelling, where the group with 1% CNF shows a reduced thickness swelling compared to the reference specimens. This group also shows a 10% improvement at internal bond strength, whereas the group with 3% CNF shows reduced internal bond strength. The same effect can be seen in the results of the bending strength, the fracture energy and the fracture toughness. For the fracture mechanical properties the improvement of the group with 1% CNF are even clearer, i.e. the fracture energy increased by 20% and the fracture toughness by 28%. For fracture toughness, the ANOVA test showed a statistical significance. Compared to the previous study of Veigel et al. (2011), a higher variation of the mechanical properties of the reinforced specimen can not be found in this study. The authors assume that the reason for the weak performance of the group with 3% CNF is not due to the high CNF content, but because of the long drying time (12h) after the glue application. Hence, it can not be said that 1% CNF is the optimum amount, but further studies should be done on this. Like in the particle board tests, the thickness swelling of reinforced OSB boards decreased. All mechanical properties show a significant improvement by adding 1% of cellulose nanofibrils (Veigel et al. 2012).

What these three previous studies have in common is that the authors conclude that cellulose nanofibrils are feasible to reinforce and / or toughen a urea-formaldehyde joint between two solid wood parts and wood based panels (Eichhorn et al. 2010; Veigel et al. 2011; Veigel et al. 2012), but none of these studies can explain this effect. One approach is that in bondline areas with high shear stress concentrations (Müller et al. 2005), the cellulose nanofibrils carry the peak forces and therefore eliminate the weak spots in the bondline. Another approach of a researcher at Wood K plus is that the cellulose nanofibrils hinder the adhesive to penetrate the wood as much as without the additive. And as a consequence, there is more adhesive in the bondline. This is the hypothesis this master thesis is based on. This hypothesis could be especially true for wood based panels like particle boards, where it is not the case that two geometrical designed surfaces are attached together, but, depending on the density and the compression factor, two particles touch each other just on certain points. Hence, more adhesive in the bondline could have a positive influence.

In the framework of a research project, Wood K plus produced three different types of particle boards, reference particle boards, boards with cellulose nanofibrils as an additive and boards with an additive that can not be further described here and is following named additive II. The boards with additives showed better results in the internal bond strength compared to the reference board. This result goes hand in hand with the studies of Veigel et al. (2011; 2012). Based on these results the objective of this master thesis was to prove or falsify the stated hypothesis, with the novel method of adhesive detection. The research was carried out on the particleboards produced by Wood K plus. Thus, the production process, mechanical testing and the results of these particleboards are described shortly in the next chapter.

2 Preliminary work by Wood K plus

2.1 Particle board production

A single layered particle board with a desired density of 650 kg/m³ (in standard climate) was produced. The raw material was industrial used middle layer particles with a portion of recycling wood and was provided by FRITZ EGGER GmbH & Co. OG. The wood moisture of the particles was 4,24%. The adhesive was a urea-formaldehyde resin named Prefere 10F133, with a solid resin content of 66%. As a hardener 3% of ammonium nitrate, based on solid resin content, was used. The hardener solution had a solid content of 60%. For these particle boards an adhesive amount of 7% (solid resin based on absolutely dry particle) was chosen and a moisture content after gluing of 11.8% was focused.
Next to the standard particle board (reference board), two types of particle boards with different additives were produced. The first additive was nanocellulose (NC) from the company Daicell (Japan). The dry matter content of the nanocellulose was 10%. The concentration of nanocellulose in the particle board was set to 5% of dry matter nanocellulose referred to solid resin content. The second type of additive was the so-called additive II. Due to a recently ongoing project with a company and the resulting confidentiality no detailed information about this additive can be given. With 7%, the dry matter content in the suspension of additive II was lower than compared to the nanocellulose additive. For reinforcing the adhesive system with additive II, 1% of dry matter based on solid resin content was added. The application of the adhesive was performed in a ploughshare mixer as it is pictured in figure 1. Figure 2 shows the interior view of the ploughshare mixer. The ploughshare mixer was filled with the particles and then switched on. In the next step the adhesive-hardener mixture was slowly added to the particles, as a thin filament out of the beaker glass. This process took around one and a half minute. The following process step differs between the reference board and the reinforced boards. In case of the reference board, water was slowly added to achieve the wanted moisture content after gluing of 11.8 %. For the nanocellulose reinforced boards, the additionally needed water was added with the nanocellulose. 1 cm³ big clusters of nanocellulose (containing water) were put into the ploughshare mixer. The addition of additive II was done in the same way than the nanocellulose.

Fig. 1: total view of ploughshare mixer (Photo credit: Stefan Pinkl)

As all ingredients were added, the mixer ran for another ten minutes to gain a proper mixture of adhesive, water and additives. The mixing in a ploughshare mixer works based on wiping effects. In the next step the glued particles were spread on a sheet of steel within a wooden frame. The wooden frame determines the size of the board, in this case 50 cm x 43 cm. After the distribution of the particles, the particle cake was pre-pressed with a wooden board, to achieve stability for manipulation into the press. The thickness of the boards was 14 mm. To enable a faster closing of the press, distance bands out of steel were used. The boards were pressed at a temperature of 220°C for the period of 140 seconds. This time was calculated with the pressing factor of 10 sec/mm. After the pressing, the boards were stored in a vertical position to cool down and to avoid buckling. Finally the panels were stored for one week in standard climate (20±2°C, 65±5 % relative humidity) for an even moisture distribution.

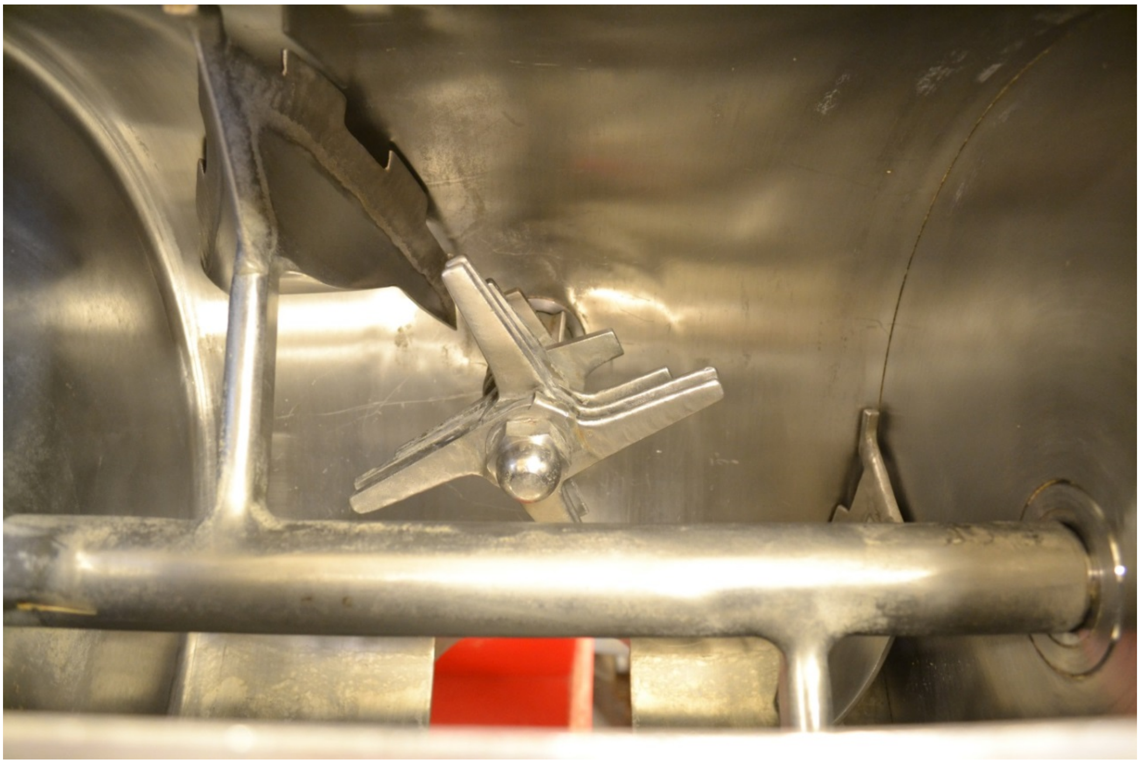

Fig. 2: interior view of ploughshare mixer (Photo credit: Stefan Pinkl)

2.2 Mechanical testing

The internal bond strength was tested based on EN 319 (1993). Therefore the particle board specimens were glued on aluminium-cross-heads with the cyanoacrylate glue Loctite 431. The testing was operated path-controlled, so that the maximum force could be achieved in 60±30 seconds. Specimens where the crack occurred in the superglue-bondline between aluminium-cross-heads and particle boards were not valid.

2.3 Results

To compare the different adhesive systems, mean values of the internal bond strength were calculated. In order to be able to compare strength values of different particle board specimens, it first had to be ensured that there was no significant difference in density of the different particle boards. Mean values of the densities are shown in table 1. A one-way analysis of variance (ANOVA) with a level of significance of 5 percent was carried out in SPSS. But because the requirement of homogeneity in variance was not fulfilled, this test was not valid. As a consequence. the Kruskal Wallis test, which is immune to inhomogeneity in variance, was used. The Kruskal Wallis test showed that there was no significant difference in the density of the different systems. But even if there is not a statistical significant difference in the density, small differences in the density still exist. Because there is a positive correlation between internal bond strength of particle boards and density, the remedial action of the so-called density correction was carried out. Density correction means that the native value is multiplied by the targeted density (650 kg/m^3) and divided by the actual density of the specimen. Hence the internal bond strength of a specimen with a higher density than the targeted is proportionally reduced and vice versa. The mean values of the density corrected internal bond strength values and their standard deviation are pictured in figure 3. The lowest internal bond strength shows the particle boards without reinforcement in the urea-formaldehyde adhesive system, with a strength of 0,465 ± 0,101 MPa. The boards with urea-formaldehyde resin plus an additive show a much higher internal bond strength, to be specific 0,628 ± 0,063 MPa for nanocellulose as additive and 0,695 ± 0,076 MPa with additive II. Thus the requirements in strength of 0,35 MPa of the standard EN 312 (2003) are fulfilled by all board types. Again a one-way ANOVA was applied with a 5 percent level of significance. This time all requirements of the ANOVA were fulfilled. The zero hypothesis, which states that there is no difference in the mean values, could be rejected. But as the ANOVA does not give information about which groups differ from each other a following Scheffé – test was applied. This test reveals that there is a significant difference between the mean values of UF and UF+NC and as well as UF and UF+AD2. This means that the internal bond strength of boards with additives is significantly higher compared to the reference board. No significant difference after a Scheffé – test can be found between UF+NC and UF+AD2, although the mean value of UF+AD2 is about 11 percent higher than UF+NC.

Table 1: Mean values of specimen densities of different adhesive systems: urea-formaldehyde, urea-formaldehyde + nanocellulose, urea-formaldehyde + additive II.

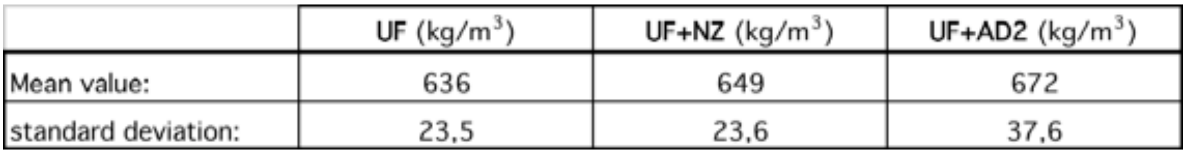

	UF (kg/m^3)	UF+NZ (kg/m^3)	UF+AD2 (kg/m^3)
Mean value:	636	649	672
standard deviation:	23,5	23,6	37,6

Abbreviations: **UF** urea-formaldehyde, **UF+NC** urea-formaldehyde plus nanocellulose, **UF+AD2** urea-formaldehyde plus additive II

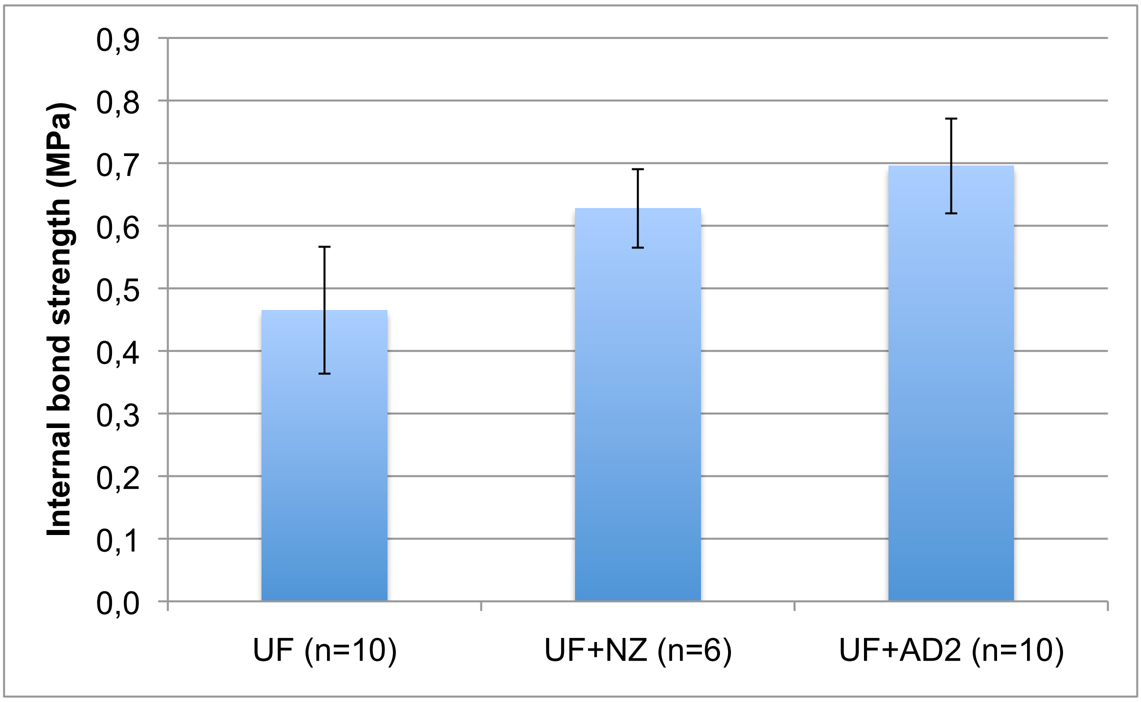

Fig. 3: Density corrected internal bond strength mean values with standard deviation of particle boards with different adhesive systems: urea-formaldehyde (UF), urea-formaldehyde + nanocellulose (UF+NZ), urea-formaldehyde + additive II (UF+AD2).

2.4 Conclusion

Particle boards with additives, e.g. nanocellulose, for reinforcing the urea-formaldehyde resin show significantly higher internal bond strength compared to the reference board. No significant difference could be found between the two additives. One reason for this might be the small sample size for UF+NC. The sample size in general for all three types is quite low and therefore tests with higher sample sizes should be carried out. But for a first assessment of the potential of different additives this study is well-suited. The intriguing question now is the reason for this enhancement in internal bond strength. Whether it is based on the reinforcing factor of the brittle urea-formaldehyde resin or on the changed distribution of the adhesive is shown in this master thesis.

3 Method

The method of adhesive detection is based on the differentiation of the adhesive in the particle boards in three different types:

- penetrating adhesive
- adhesive in the bond line
- free adhesive

A schematic representation of this classification is shown in figure 4.

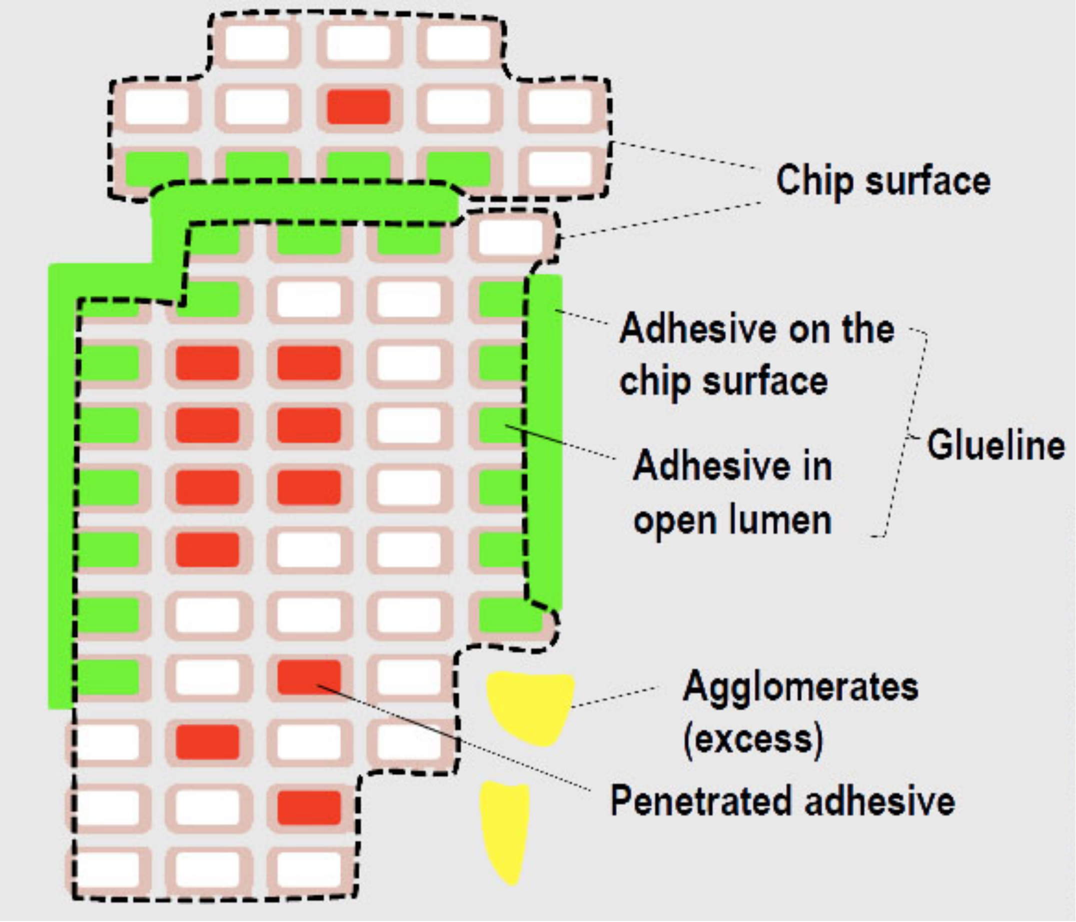

Fig. 4: Schematic representation of the classification of the adhesive in particle boards. Created by Ulrich Müller (Van Herwijnen et al. 2013).

To make the determination of these three different types possible, it was necessary to prepare stained thin slices out of the specimen in the first step. Once this was done, close-up pictures could be taken under the microscope. Subsequently different steps of image editing followed, before the different portions of adhesive could be calculated. This chapter gives a detailed insight in the method of adhesive detection step by step.

3.1 Sample preparation

The samples for preparation of the thin slices were taken from the bending test specimens. For this reason thin stripes of an approximate thickness of 3-4 mm were cut off the bending test specimens in longitudinal direction, as shown in figure 5.

Fig. 5: Thin stripes of bending test samples where 3 x 4 mm cubes were cut out.

Of each type (reference, NC, additive II) stripes of two different bending test specimens that were cut out of two different panels were provided. Subsequently, of each board in total ten small pieces with a size of approximately 3 x 4 mm were cut out with a razor blade (Figure 3). The places where they were cut out were chosen randomly. The only criteria were that the area should be densely pressed and without any gaps. In the next step the small particle board cubes were impregnated with epoxy resin to achieve good stability of the thin slices. The used epoxy resin was an Agrar Low Viscosity Resin (LV). For this process the cubes were put in an ampulla which was filled-up with epoxy resin. The ampullas were put into the exsiccator and vacuum was applied for app. 20 min. Then atmospheric pressure was slowly re-established to ensure that epoxy resin could penetrate even into small pores. This procedure was repeated once, so that no air bubbles were rising any more. After that the resin-penetrated cubes were put in a silicone form for embedding with epoxy resin. The embedding happened in the same position as they were cut out of the stripes. The epoxy resin had a curing time of 16 – 24 hours at a temperature of 60°C. In the next step a 1 mm thick disc had to be cut out of the embedded sample. Ergo the embedded samples were glued on a special wooden strip with a 2k-epoxy-resin. Subsequently the 1 mm discs were cut out with a sample-disc-cutter. The already cut samples on the wooden strip are shown in figure 6.

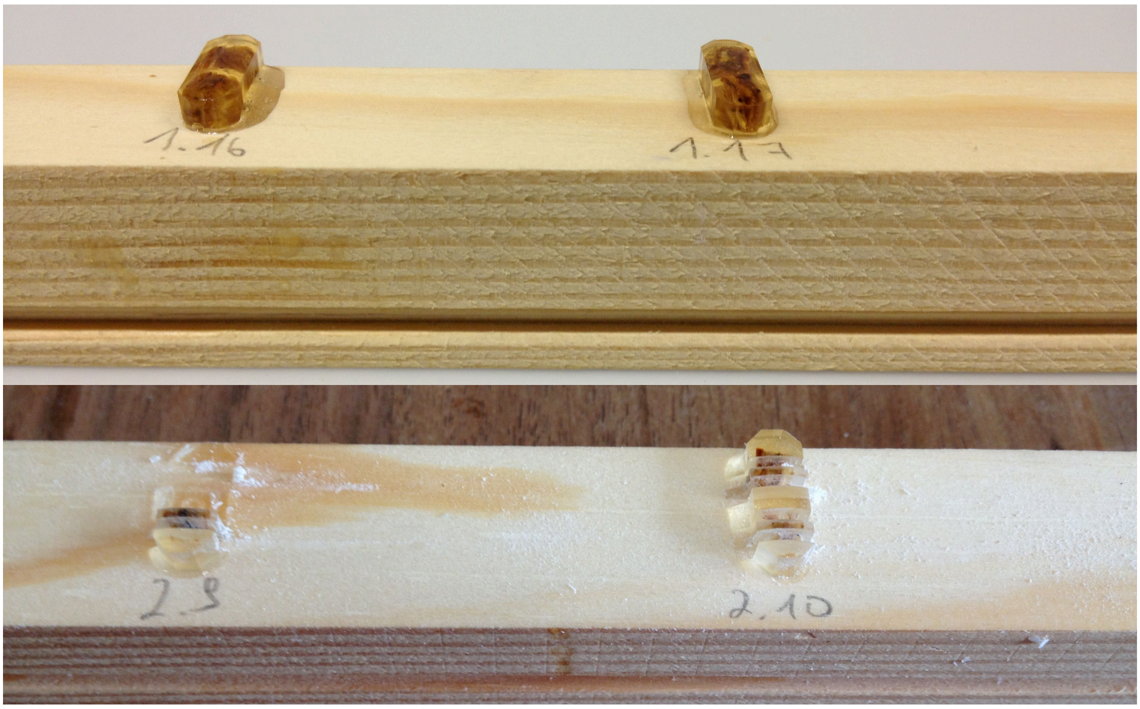

Fig. 6: Embedded samples glued on wooden stick (top) and already cut (below).

The 1 mm thick discs were subsequently glued with a 2k-epoxy-resin on a cylindrical carrier out of brass, hence it could be fixed in the Leica Ultracut-R for production of the thin slices. For creating thin slices, a smooth surface had to be produced first of all. Once this was accomplished, thin slices with a thickness of 2000 nm were produced with a Diatome Histo diamond knife. The thin slices glided in a small water bath where they swam on the surface and could further be manipulated for staining. In the first staining step the sample was stained with a fluorescent agent called Brilliant Sulphaflavine. This substance was chosen because it works best for detecting UF resin on wood according to Riegler et al. (2012). This agent stains the complete sample, the wood matter, the adhesive and the epoxy resin. For this step the thin slice was taken with a pair of tweezers and was put on the surface of the fluorescent agent, a 0.1% solution of Brilliant Sulphaflavine, for approximately one minute. After this the thin slice was put on the surface of clean distilled water to remove the spare fluorescent agent. The thin slice stayed on the water surface for approximately 10 minutes before it was manipulated with a cover slip on the microscope slide. Between the covering slip and the microscope slide, there was a droplet of water then which had to evaporate for about half an hour before the next staining step could be started. The stain Gentianaviolet that was used for this step, adhered to the wood substance but not to the urea-formaldehyde resin. This means that it covered the fluorescence molecules on the wood matter and subsequent only the UF-resin was visible under fluorescent light. The 0.2% solution of Gentianaviolet was put in small droplets next to the covering slip and due to gravitation it flowed between covering slip and microscope slide and stained the thin-layer cut. Furthermore it was possible to increase the flow of the staining agent by holding some paper on the opposite side (to the droplet of Gentianaviolet) of the covering slip, the paper got soaked and thus a flow under the covering slip was created. This step was repeated until the whole thin slice was stained. The last step of the staining process was to wash out the spare staining substance. Droplets of distilled water were put next to the covering slip and with a paper on the opposite side, a flow was created which slowly washed out the spare staining substance. The thin slices needed to be dried completely with the absence of light, before they could be used for the microscopy. Of each sample two thin slices were produced for the reason that some thin slices were useless for the microscopy because of mistakes or insufficient work of staining process e.g. too little fluorescent pigments.

A microscope of the type Axioplan 2 from the company Zeiss was used. For the fluorescence microscopy the microscope is equipped with an ultraviolet lamp of the type FluoArc HBO 100. The aim of the microscopy was to create a complete picture of the thin slice with a 100 x magnification. Because of the high magnification it was not possible to achieve this picture with one shot, as a consequence the thin slice was grid-like photographed. To be able to determine the different adhesive portions, photos under halogen light (figure 7) and fluorescent lights (figure 8) were necessary. The photo series always started with a picture under halogen light. Then the light source was changed to fluorescent. This change had to be enacted with caution so the position of the sample was not changed unintentionally, because these two pictures had to be matched again later on. Before taking the picture some adjustments of the parameters needed to be done. Then the position was changed and the next picture was taken. When changing the position for the next image it had to be considered that a small overlapping area was always necessary for combining the images later on. Depending on the size of the thin slice, the sample was divided in a raster of 3 x 3 or 4 x 4. This means that for every thin slice a total amount of 18 – 32 pictures had to be taken.

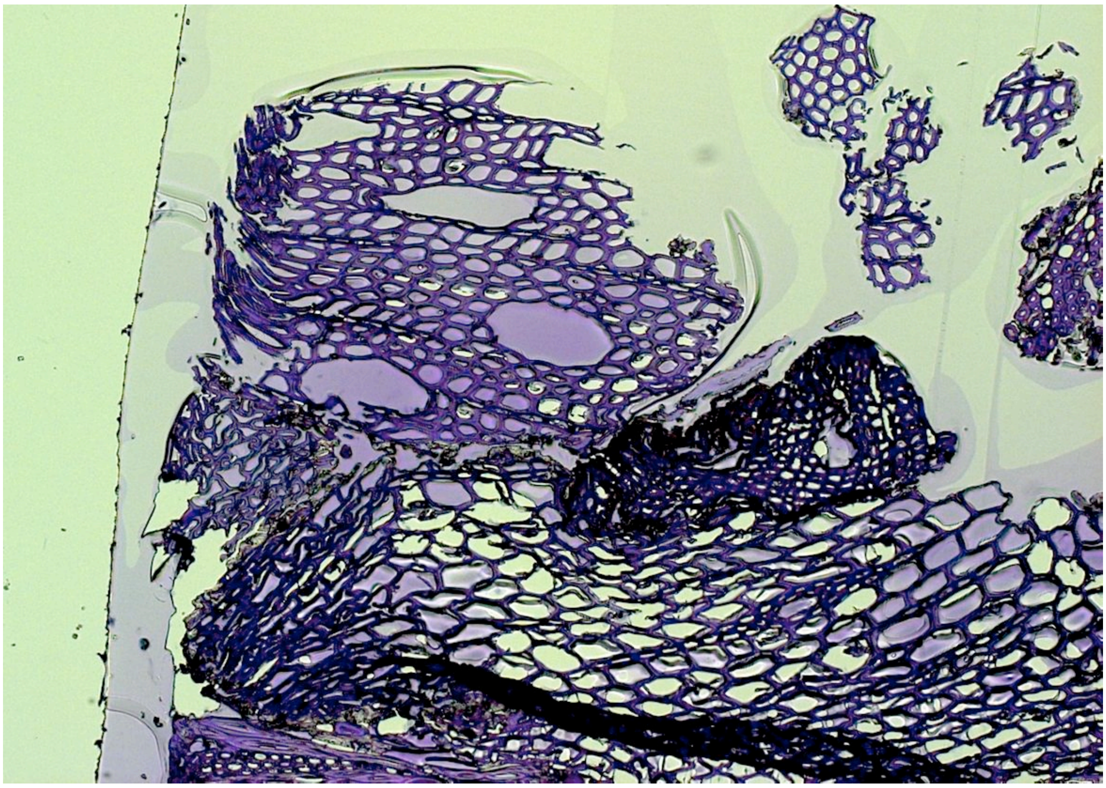

Fig. 7: Image under halogen light with 100 x magnification. Dark violet areas are wood matter. Violet areas in the lumen are not properly washed out spare stain.

Fig. 8: Image under fluorescent light with 100 x magnification. Bright areas or spots are either epoxy resin, urea-formaldehyde resin or not properly with Gentianaviolet covered other material.

3.2 Image editing

To get the final files with which the analysis of the adhesive distribution is possible, several image editing steps in Photoshop were necessary. They are explained in this chapter step by step:

3.2.1 Step 1: Differentiation between adhesive and other fluorescenting spots

As already mentioned in the description of figure 8 not only the urea-formaldehyde resin is fluorescenting in the microscopy image under fluorescent light. Actually everything of the thin slice matter is glowing under fluorescent light that is not covered by the Gentianaviolet stain. Since none of the staining processes ever worked out perfectly there was always some matter glowing that should not glow. Depending on the position of the image (edge or inside) more or less “unwanted” bright spots appeared. Images on the edge of the thin slice sample always showed a great amount of bright spots / areas due to the epoxy resin in which the thin slice was embedded. The fluorescent molecules of the Brilliant Sulphaflavine stuck to the epoxy resin but were not covered by the Gentianaviolet. The bright glowing epoxy resin can be seen in figure 8. The objective of this first editing process was to eliminate all the glowing spots that are not adhesive in the opinion of the scholar. This was, next to the determination of the particles, the most important process step in the adhesive detection method. The decision whether something is adhesive or not, was not always clear and required a lot of sense and personal evaluation of the scholar. To achieve comparable and reproducible results it was of high importance that this step was performed by the same researcher for all specimens. Nevertheless there are a few points that need to be considered and helped in the decision-making:

- Bright areas on the brink of the thin slice are always epoxy resin. Due to fine cracks epoxy resin can also be found on the inside of the sample.
- Bright areas on the brink of a particle are in the majority of the cases adhesive.
- Bright areas on the inside of a particle should look like a moonscape with craters to be declared as adhesive.
- Adhesive appears slightly yellow on the halogen-light image.

For this first process step both the halogen image and the fluorescent image were opened in Photoshop. Then the layer of the halogen image called

Hintergrund was duplicated in the document of the fluorescent image. This could be done in the layer control panel. Now, the halogen image laid above the fluorescent image and it was possible to change the opacity of the top-layer namely the halogen image with the scroll bar. This was a necessity of the first processing step. To decide whether some bright spots are adhesive or not the opacity must always be changed between 0% and 100%, e.g. to see if a bright spot is located in the bondline or whether it appears slightly yellow. If the opinion was built up upon a bright spot that is not seen as glue it had to be erased. Therefore the layer of the fluorescent image was highlighted and the bright spot was painted over in black colour with the brush tool. If all unwanted bright spots were erased the opacity of the halogen image was set to 16 percent and the document was saved as a .tif-file in a new folder. The outcome of this process step is shown in figure 9. Before it was possible to move on to the next step, this editing had to be done for all grid-images.

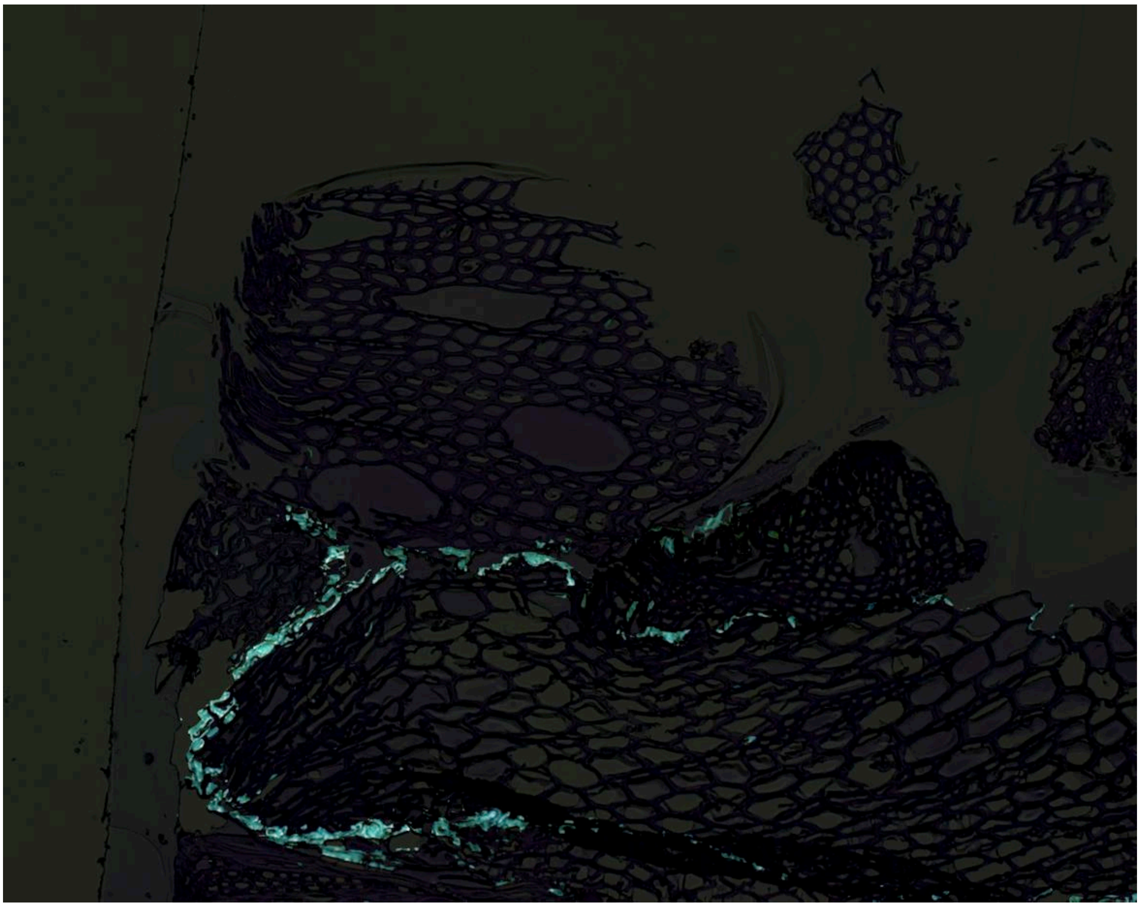

Fig. 9: Combined halogen (with opacity of 16 %) and fluorescent image after first image editing step. All bright spots which were not declared as adhesive had been erased. Remaining bright spots are seen as adhesive.

3.2.2 Step 2: Assembling of images

As mentioned before, the thin slices were photographed grid-like due to the small field of view. To get one whole image, the single images had to be combined again. For this step, an add-on of imageJ, the so-called mosaicJ, was used. All single images of one thin slice were loaded into mosaicJ and were then assembled manually. To make this possible it was necessary to always have some overlapping area when making the images under the microscope. The outcome of this processing step is a mosaic and a picture of the whole thin cut, shown in figure 10.

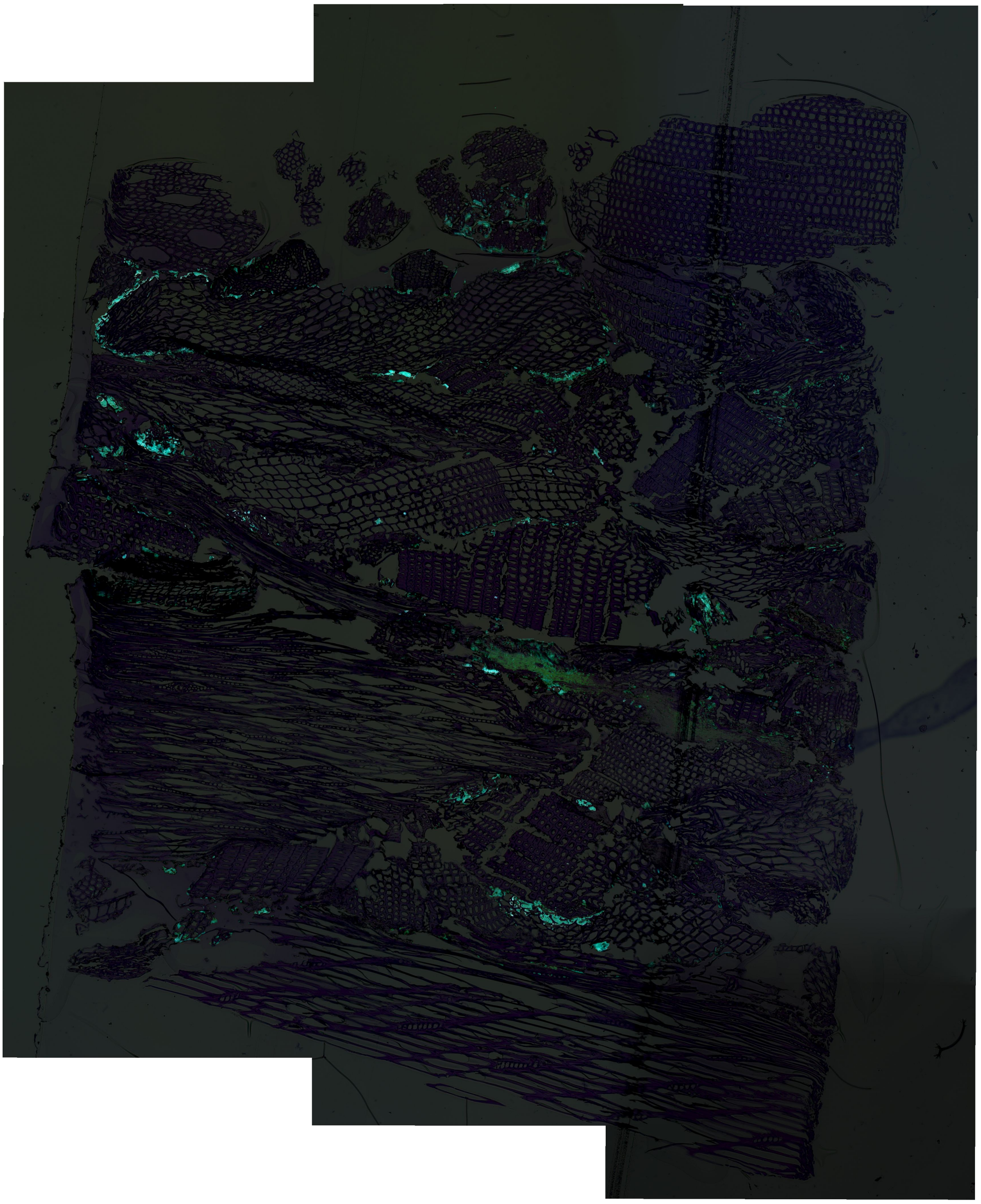

Fig. 10: Image of a whole thin slice after assembling the single images with mosaicJ. Bright spots are adhesive, dark violet areas are wood matter.

For closing this process step the mosaic image was saved in a new folder.

3.2.3 Step 3: Retracing the particles

As already mentioned before, after the determination of the adhesive the retracing of the particles was the most important step. Accurate proceeding was of high importance in this step, due to the fact that this process step determines which parts of adhesive are either in the bondline or penetrated. The bondline was set to have a width of 25 μm in this method.
First of all the mosaic image had to be opened in Photoshop. For the following analysis of the adhesive distribution the mosaic had to be surrounded by a black frame, so the working area was increased by 500 Pixel in height and width. This was done in the menu *Bild → Arbeitsfläche.* In this menu *Pixel* was set as unit and also the menu-point *relativ* was selected. Subsequently the size of the working area could be increased. The frame around the mosaic appeared in white colour. With the tool *Zauberstab* the white area was selected and then coloured black with the tool *Füllwerkzeug.* As another preliminary step several layers had to be compiled before retracing could be started. First of all a copy of the layer *Hintergrund* with the name *Hintergrund Kopie* had to be generated and also three new empty layers with the names *Leimfuge*, *Leimfuge Schnitt* and *Span* had to be be generated. The reason for this will be explained later. The new layer *Hintergund Kopie* could then be brightened up for a better detection of the particles. Following steps for brightening were necessary: menu *Bild → Korrekturen → Helligkeit/Kontrast*. The particles were retraced on the layer *Hintergrund Kopie* with the tool *Polygon-Lasso-Werkzeug*. For retracing the particles it is recommended to use a high magnification so that each border of the particles could be retraced as accurately as possible. Even open lumina should be retraced accurately. After all particles had been retraced, the drawn bondline had to be filled. The filled bondline must be in a separate layer, so the layer *Leimfuge* was highlighted. For filling up the bondline a right mouse click in one of the retraced particles was done and the menu point *Kontur füllen* was chosen. Subsequently the setting for the bondline appeared. A width of 25 Px (that equals 25 µm) was chosen, the colour red selected and the position was set to *middle*. After clicking the *OK-button* and *Strg-D* the red bondline appeared and the interrupted line disappeared. Figure 11 shows how the complete document with all layers visible looks like after this step.

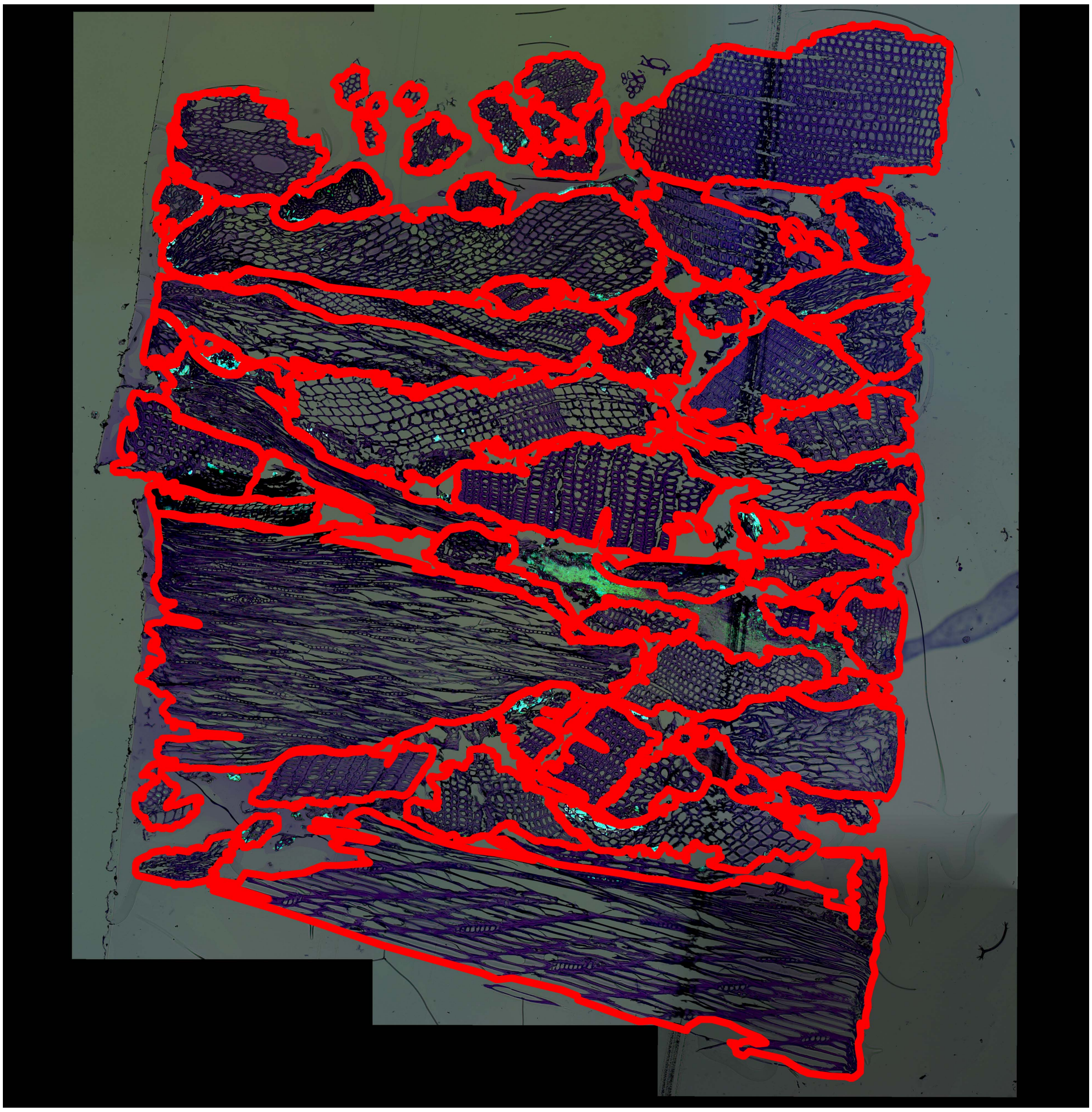

Fig. 11: Thin-cut with retraced particles. Red line is the bondline.

3.2.4 Step 4: Generating images for analysis

To analyze the location of the adhesive, several new images were created out of the mosaic image in figure 11. In step 3 a new layer with the name *Leimfuge*, where only the bondline appears, was created. Out of this layer the area of the particles is imaged in the layer *Span*. The area of the particles means everything that is surrounded by a bondline, but the bondline itself does not account as particle area. First the layers *Leimfuge Schnitt* and *Hintergrund* were made invisible. This was done in the control panel layers. In the next step the layer *Leimfuge* was highlighted. Now the mosaic image with the particles and the bondline was visible and with the tool *Zauberstab* all particles could be selected. To see the particles in the layer *Span,* this layer was highlighted and the areas of the selected particles were filled black with the tool *Füllwerkzeug* (Figure 12).

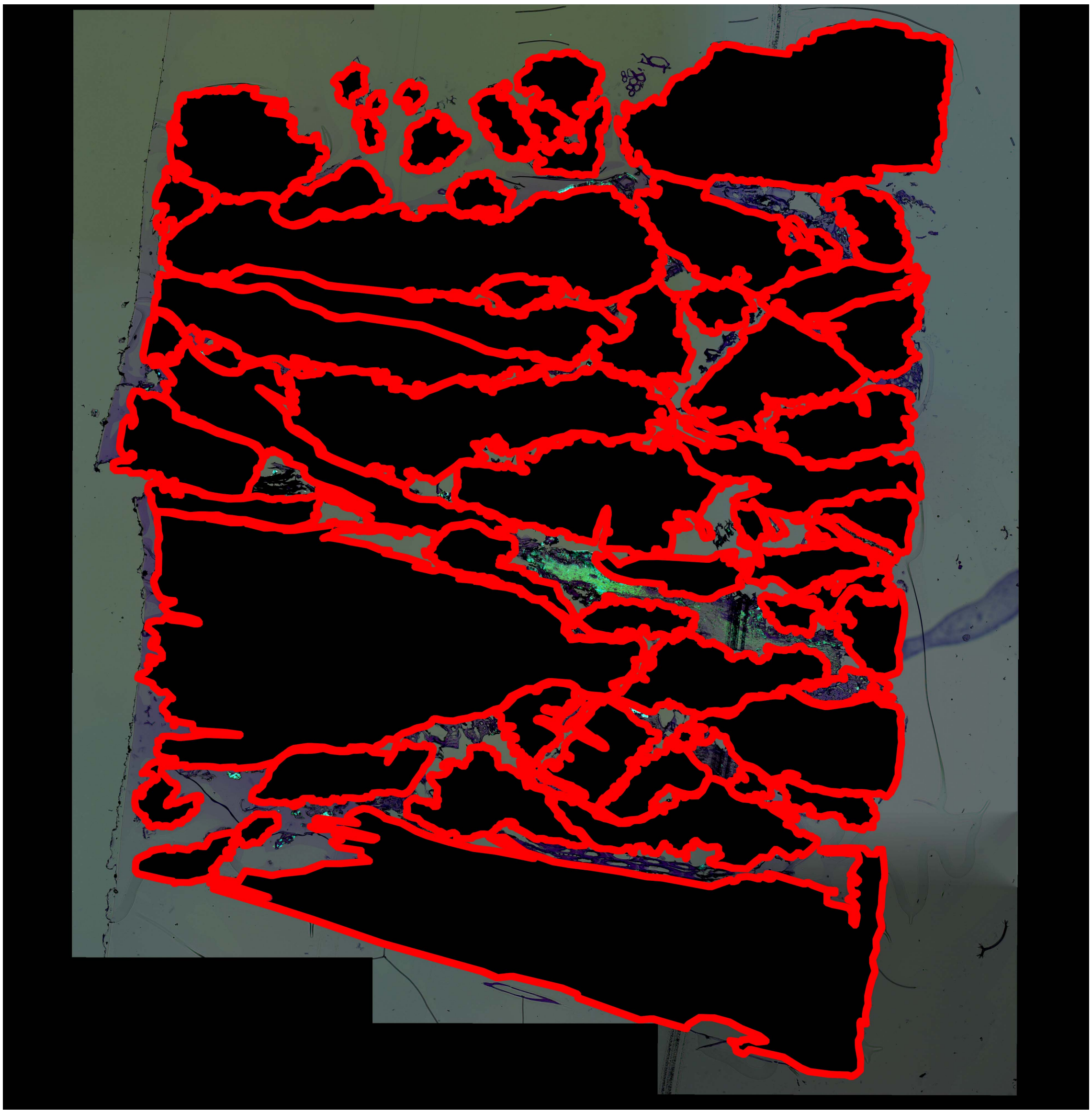

Fig. 12: Image after filling up the area inside the glue joint. Black areas are wood particles.

The next processing step was to delete the bondline that was surrounding the thin slice. This was done because of the epoxy resin the thin slice was embedded in. And as already previous mentioned, the epoxy resin is appearing in the same way as adhesive and is therefore a high potential risk of failure. The second reason was due to the preparation of the thin slice, hence the outside line of the specimen is not necessarily a bondline. But the surrounding bondline is only deleted where its course follows an imaginary rectangular frame at the border of the thin slice. This means that an outside bondline which is, due to a hollow space in the thin slice, not at the outside border of the specimen is not deleted, as figure 13 shows. First the red glue joint of the layer *Rand* was copied in the layer *Rand Schnitt*, subsequently with the tool *Buntstift* a 25 Pixel width, red tangent was drawn around the thin slice (figure 13 b). The next step was to pick the tool *Zauberstab* and click on the outside of the red line. Now the red border of the thin slice was selected. Then menu *Bearbeiten* → *Kontur füllen…* was chosen, the width was set to 28 Pixel, position was set to *Außen* and *Füllmethode – Modus: Löschen* was selected. After pressing *OK*, the outside red line was deleted, as shown in figure 13 c.

Fig. 13: Deleting outside bondline due to sample preparation and epoxy resin embedding: (a) image after particle retracing (b) red tangent was drawn for closing hollow spaces (c) outside bondline was deleted.

Furthermore, single images with just black and white information had to be exported out of this document with its several layers. The black and white transformation was necessary because the final calculation worked binary with white as zero (0) and black as one (1). The first image was the layer *Span*. Thus every layer except the layer *Span* was deleted and with the option *Bild* → *Modus* → *Graustufen* the remaining layer was converted into a black and white image. This image, as pictured in figure 14, was afterwards saved in a new folder with the name *SpanSW*. With the operating panel *Protokoll* the deletion of the other layers was reversed. Next layer was *Rand Schnitt*, and again all other layers were deleted. To get a black and white image out of the red glue joint, first of all the *Schwellenwert* was set to 255 under the menu *Bild* → *Korrekturen* → *Schwellenwert* and after that the option *Graustufen* was used again. This image was saved titled *Leimfuge* (figure 15). The final image that was needed was an image where just the adhesive was visible. This was generated out of the layer *Hintergrund*. The process worked out the same as above, deleting all layers except *Hintergrund*, menu *Bild* → Korrekturen → Schwellwert, where the *Schwellwert* was set to 80. With this *Schwellwert* value the bright adhesive areas stayed white while everything else turned black. Before it was saved with the name *Leim,* the option *Graustufen* was applied again. The adhesive as white areas is shown in figure 16.

Fig. 14: Black and white image of the particle area. Black areas are wood matter (particles).

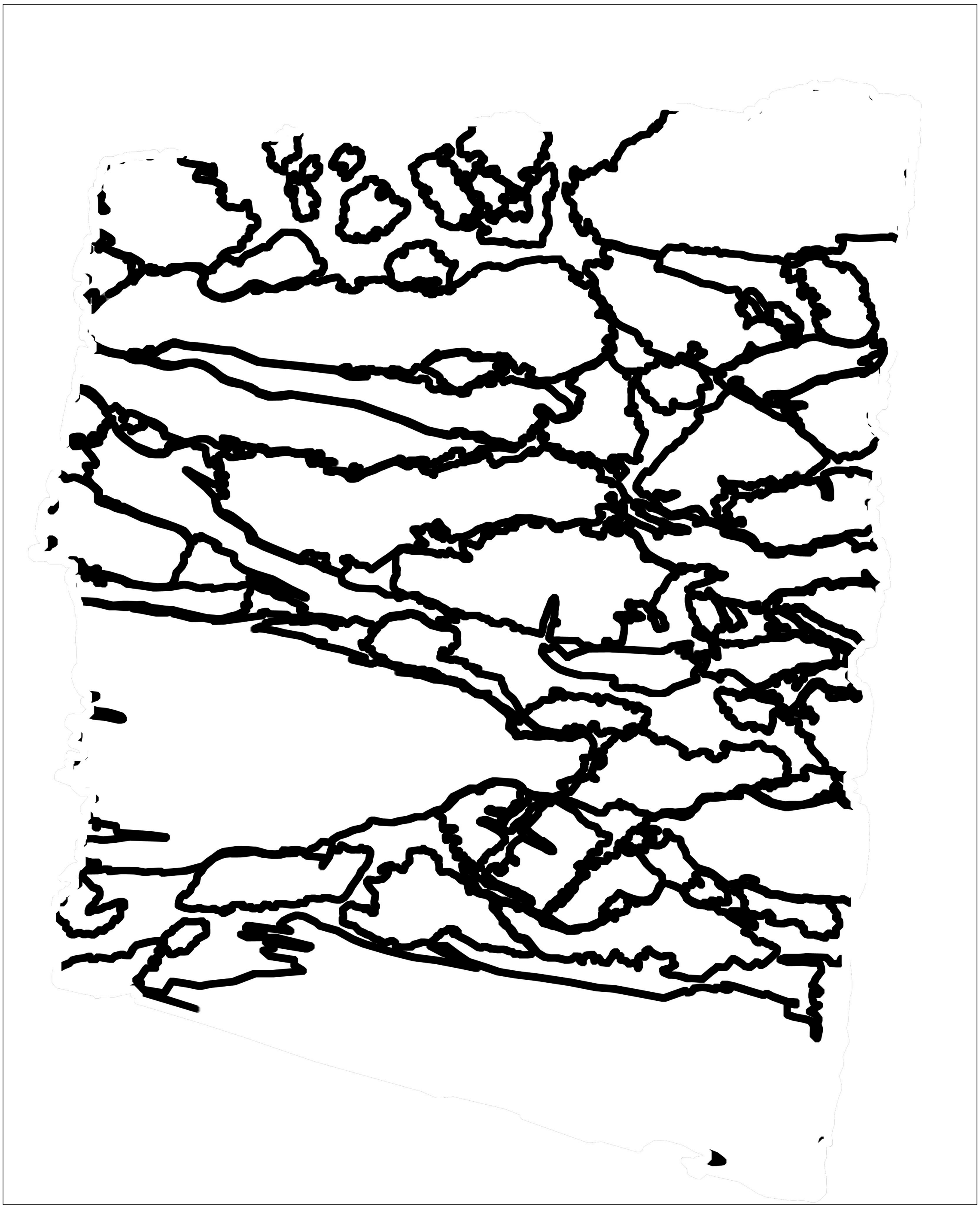

Fig. 15: Black and white image of the glue joint. Black line is the 25 µm thick glue joint.

Fig. 16: Black and white image of the adhesive. White areas are adhesive.

3.2.5 Step 5: Binary transformation and analysis of images

It was necessary to transform the images into binary coded files to analyze the location of the adhesive. This step was done for files *SpanSW*, *Leimfuge* and *Leim* in the program ImageJ and the menu *Process → Binary → Make Binary.* Hence, these binary images were saved in a new folder. The appearance of the images *Leimfuge* and *Span* was not changed through the binary transformation, but colours of the image *Leim* were inverted. The adhesive in the new binary image, that is shown in figure 17, is now appearing black. For additional analysis of the covering of the particles with adhesive the binary image *Leimfuge* was subsequently skeletonised under menu *Process* → *Binary* → *Skeletonize*. The skeletonizing process changed the 25 Pixel width glue line to a line with just 1 Pixel in width (figure 18). This line marks the border or surface of the particles.

Fig. 17: Binary coded image of adhesive. Adhesive appears now in black color.

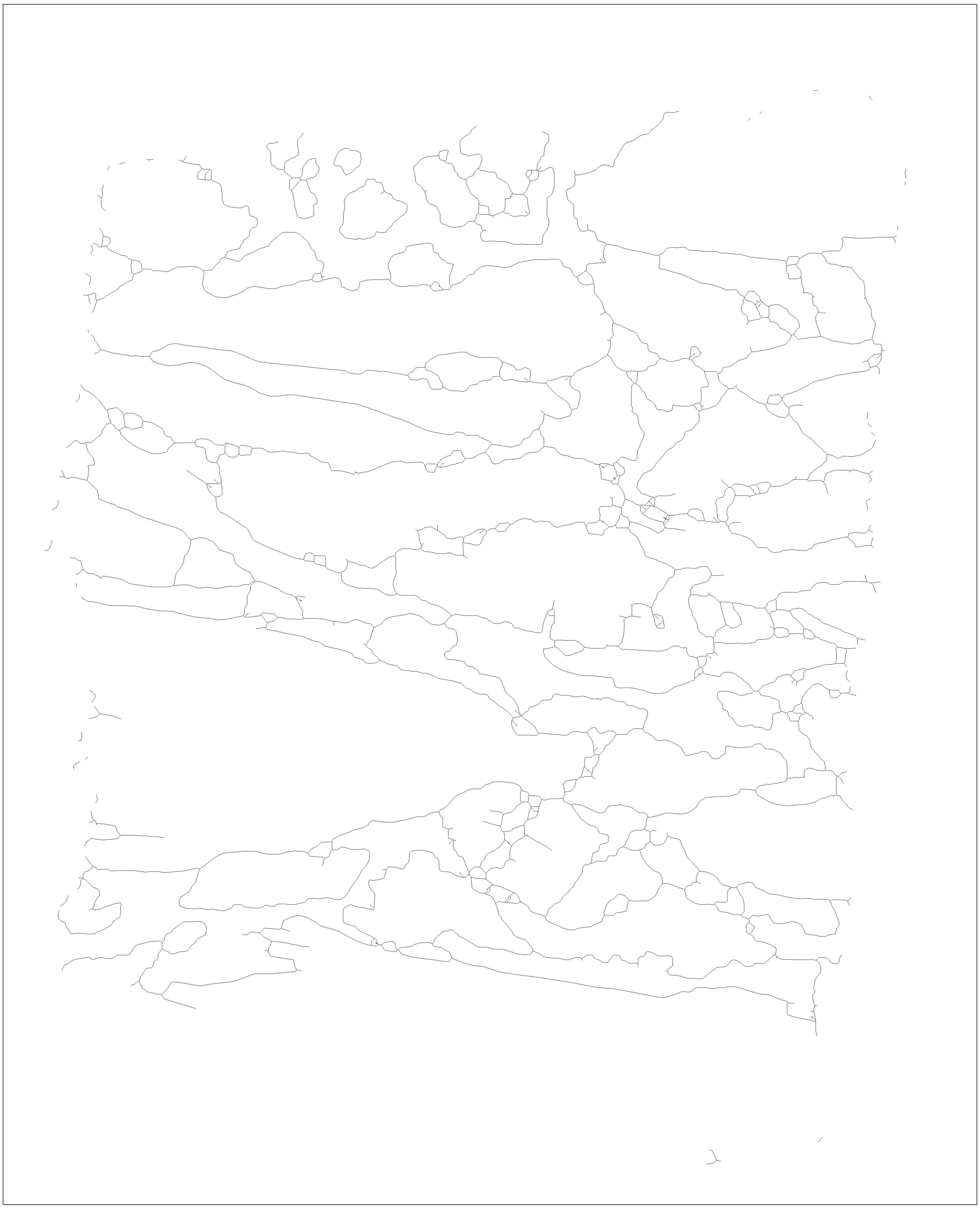

Fig. 18: Skeletonized image of the image *Leimfuge*. Black line has a width of 1 Pixel and marks the surface/border of the particles.

In the next step the scale had to be set equal for all needed images. Therefore following files were opened in imageJ: *Leim*, *Leimfuge*, *Leimfuge skeletonised* and *Span*. The scale was set in the menu *Analyse → Set Scale* with *Distance in Pixel: 1300*, *Known Distance: 1378* and a *Unit of length: µm* equals a ratio of 0.943 pixel/µm. Furthermore the menu *Global* was set.

After this was done the files that give information about the location of the glue, could finally be generated. This was made with the logic gate AND. For this reason the images had to be transformed into binary coded images. As the logic gate AND can just read zeros and ones, the colors were coded through the binary transformation: white stands for 0 and black for 1. This means that in our images everything that is of our interest is a logic 1, e.g. adhesive in figure 17, the bondline in figure 15 or the particles in figure 14. How the logic gate AND works is shown in figure 19.

Fig. 19: Operating mode of a logic gate AND (source: www.openmymind.net)

After implementing this logic in the analysis, the carried out operations worked as following for example: if a black pixel (1) of adhesive occurs in the area of the bondline, that is also represented by a black pixel (1), a black pixel is generated at this position in the new image (figure 20). This logic operation was done in *Process → Image Calculator*. Following logic operations were conducted:

- Leim AND Leimfuge	saved as: LR
- Leim AND Leimfuge skeletonised	saved as: LRSKT
- Leim AND Span	saved as: LS

It was important that image *Leim* was always set as first image. The newly generated images are shown in figure 20 and figure 21. The second image *Leim* AND *Leimfuge skeletonised* is not shown here because of too little adhesive on the particle surface / border it does not show any results.

The images of *Leim*, *Leim and Leimfuge*, *Leim and Span* as well as *Span* were finally analysed with the option *Analyse → Analyse Particles*. As settings the default settings were adopted.

It measured the size/area of the particles, adhesive in the bondline and penetrated adhesive (possible because of the scaling from pixel to micrometer).

The required results were the area of every wood or adhesive particle as well as the summary with the total particle size for the whole image, the average size and the number of particles in the image. This data was exported to an excel file and analysed.

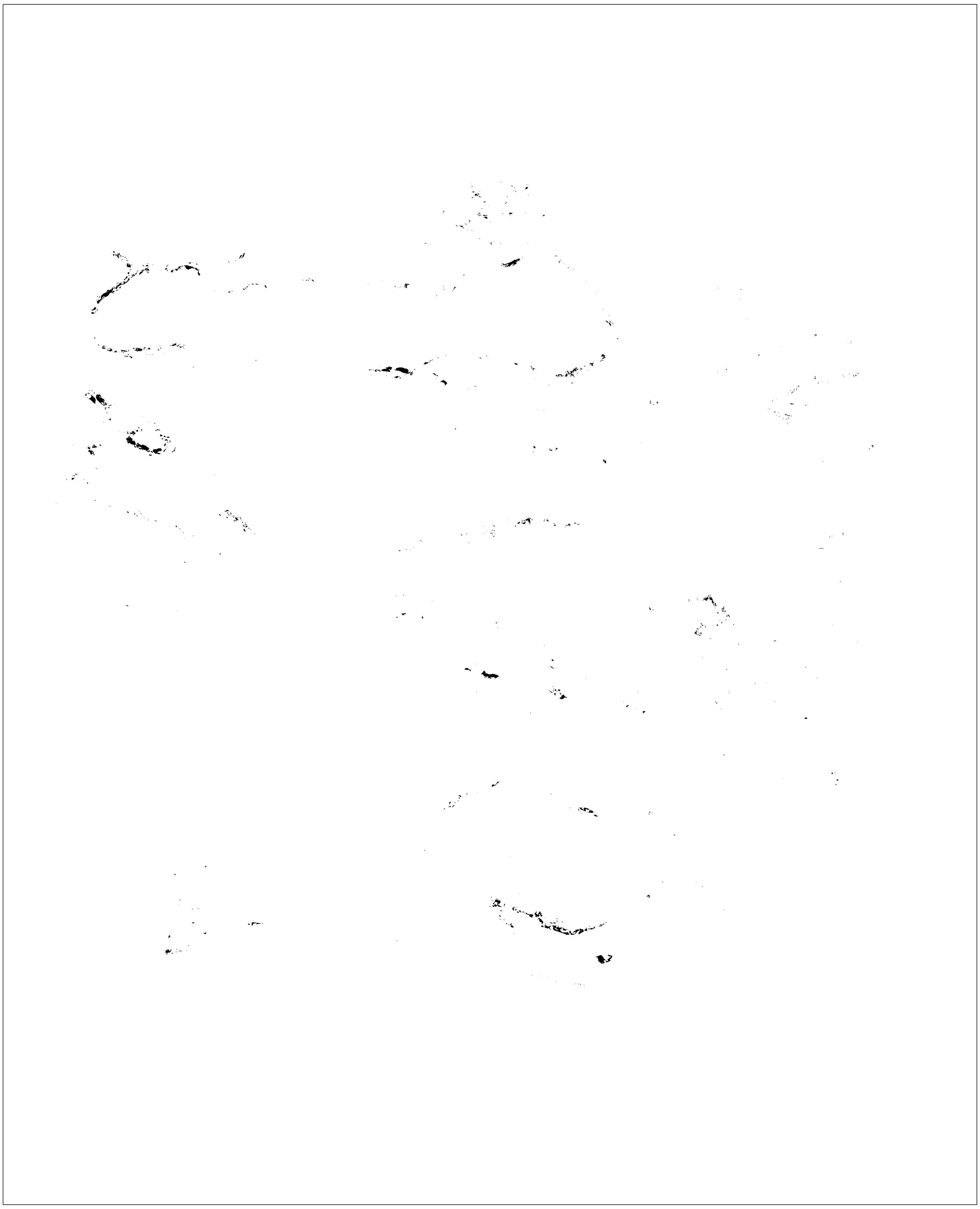

Fig. 20: New image generated with the logic function AND of the images *Leim* and *Leimfuge*. Black areas are adhesive in the bondline.

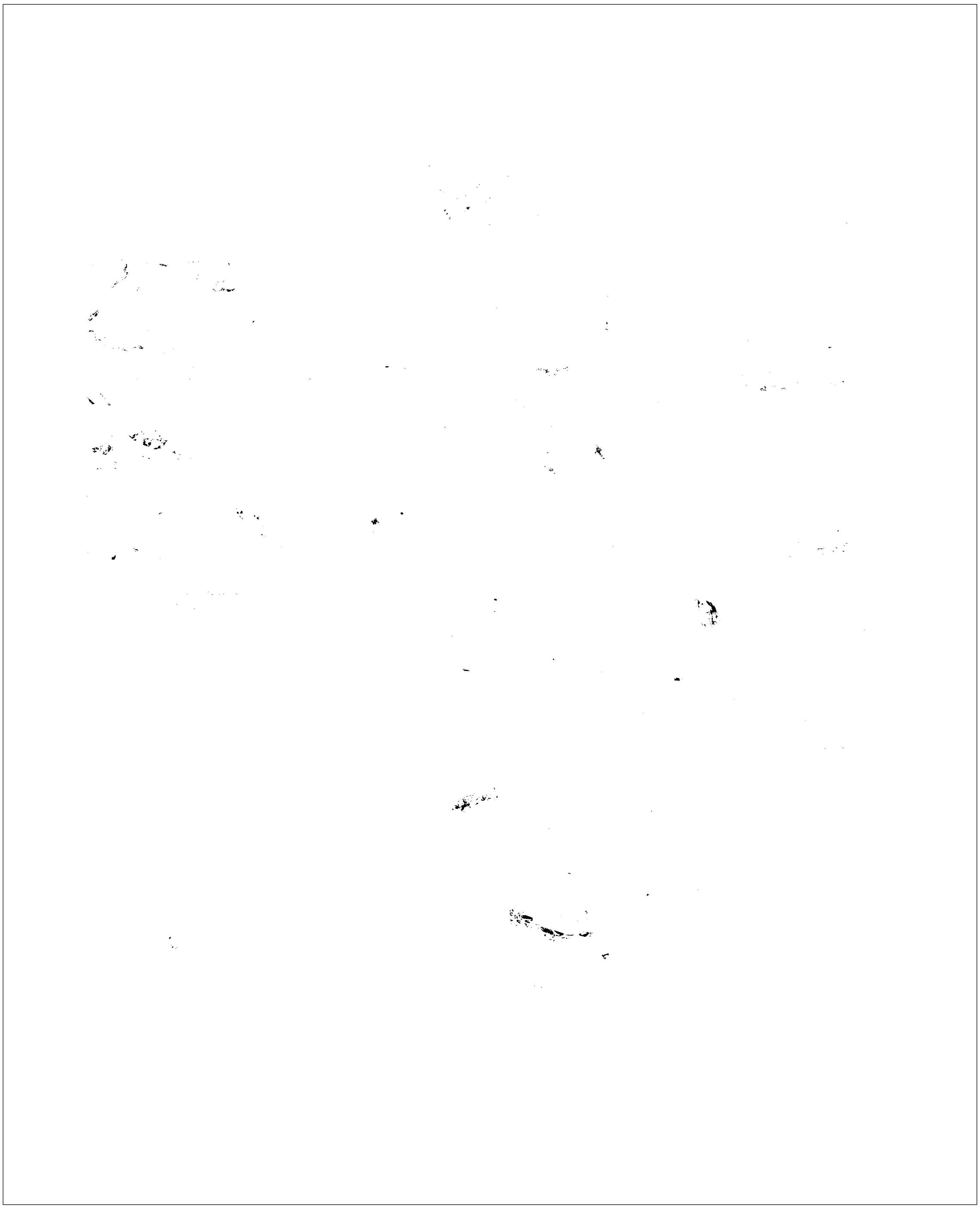

Fig. 21: New image generated with the logic function AND out of the images *Leim* and *Span*. Black areas are adhesive in the particles, also termed as penetrated adhesive.

4 Results and Discussion

With the results of the image analysis the distribution of the adhesive was calculated in Excel as follows:

$$adhesive\_bondline = \frac{LR}{Leim}$$ LR…Leim Rand

$$penetrating\_adhesive = \frac{LS}{Leim}$$ LS…Leim Span

$$Excess = adhesive\_total - adhesive\_bondline - penetrating\_adhesive$$

The results show quite a high variance, especially the specimens of the unreinforced particle boards (A1 & A2). To get an idea what the particular results of the specimen look like, they are shown in figure 22 to 24.

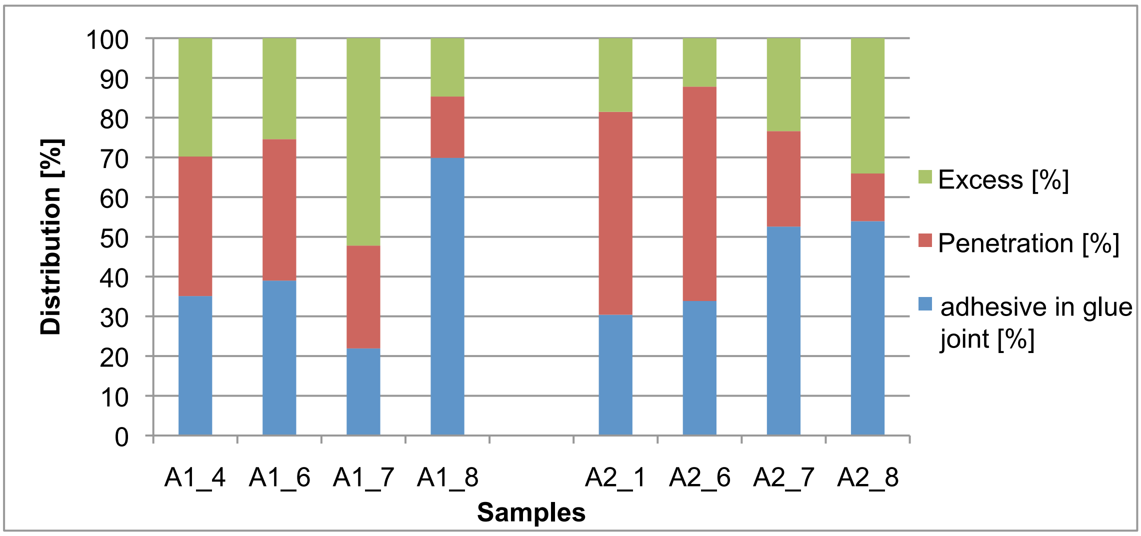

Fig. 22: Distribution of the adhesive in particle boards without additives. A1 and A2 are two different boards, but the same adhesive system.

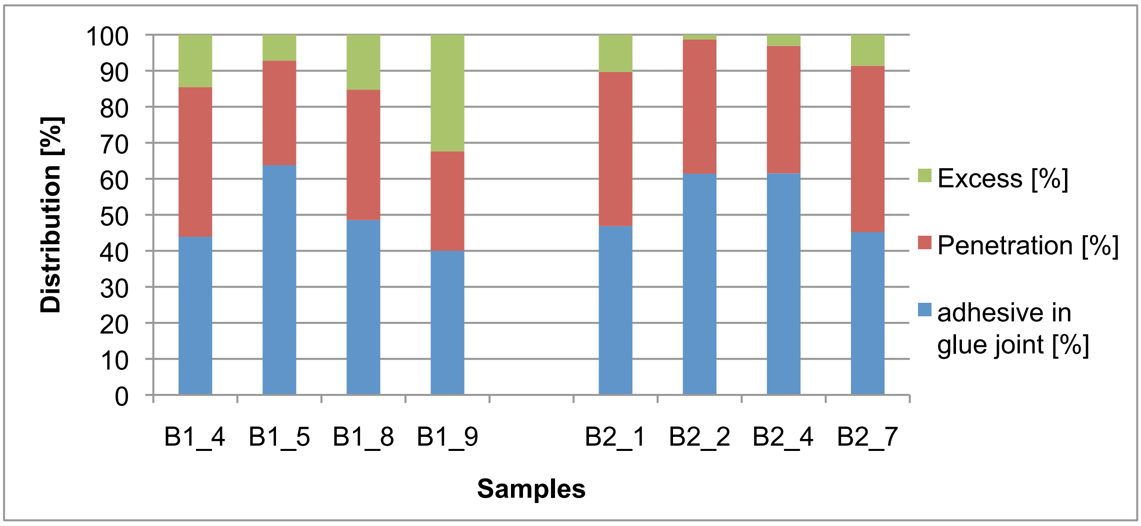

Fig. 23: Distribution of adhesive in particle boards with 5 % of nanocellulose as additive. B1 and B2 are two different boards but the same adhesive system.

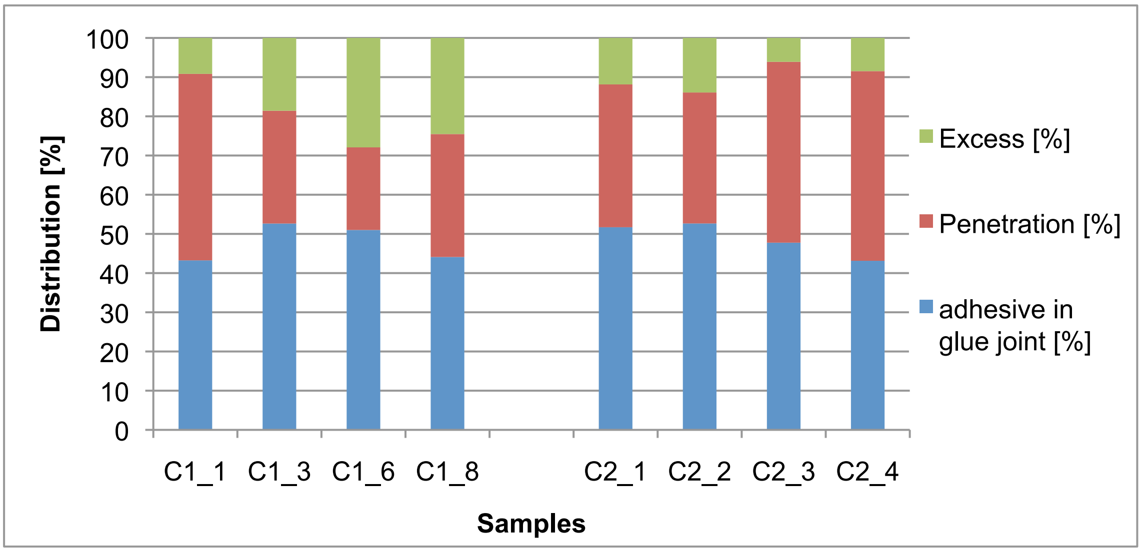

Fig. 24: Distribution of adhesive in particles boards with 1 % of additive II added. C1 and C2 are two different boards but the same adhesive system.

Despite the high variability there is a certain trend recognizable. It looks like the excess of adhesive is highest in the unreinforced adhesive system A (figure 22), while it is lowest in the adhesive system B with nanocellulose. This high excess has obviously an impact on the other two portions: adhesive in the bondline and penetrated adhesive. Hence, adhesive in the bondline looks highest in adhesive system B. This estimation is proved by figure 25, where the mean distribution values of the individual particle boards are shown.

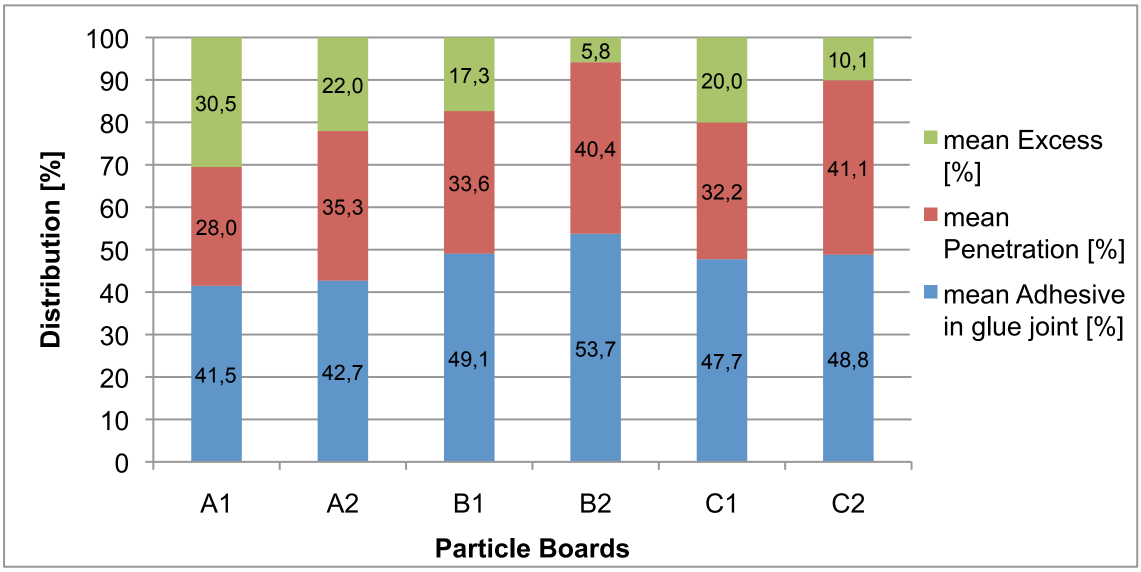

Fig. 25: Mean values of adhesive distribution of the individual particle boards: (A) urea-formaldehyde, (B) urea-formaldehyde + nanocellulose, (C) urea-formaldehyde + additive II.

Noticeable in figure 25 is that there is still a high difference in the mean values of the particle boards with the same adhesive system. And that this difference is basically based on the portions of the penetrated adhesive and the excessive adhesive, which is neither located in the glue joint nor in the particle. For example the excessive adhesive and the penetrated adhesive in C1 and C2 differ about 10% while the adhesive in the glue joint is more or less the same. Figure 26 shows the mean distribution values of each adhesive system respectively. The trend that was already seen in the individual results of the reinforced specimen, namely that there is more adhesive in the glue joint and more adhesive penetrating due to less excessive adhesive, can be confirmed with this chart. Of course it has not been proven whether it is statistically significant because of the high standard deviation (±15.6% in the worst case) at this moment.

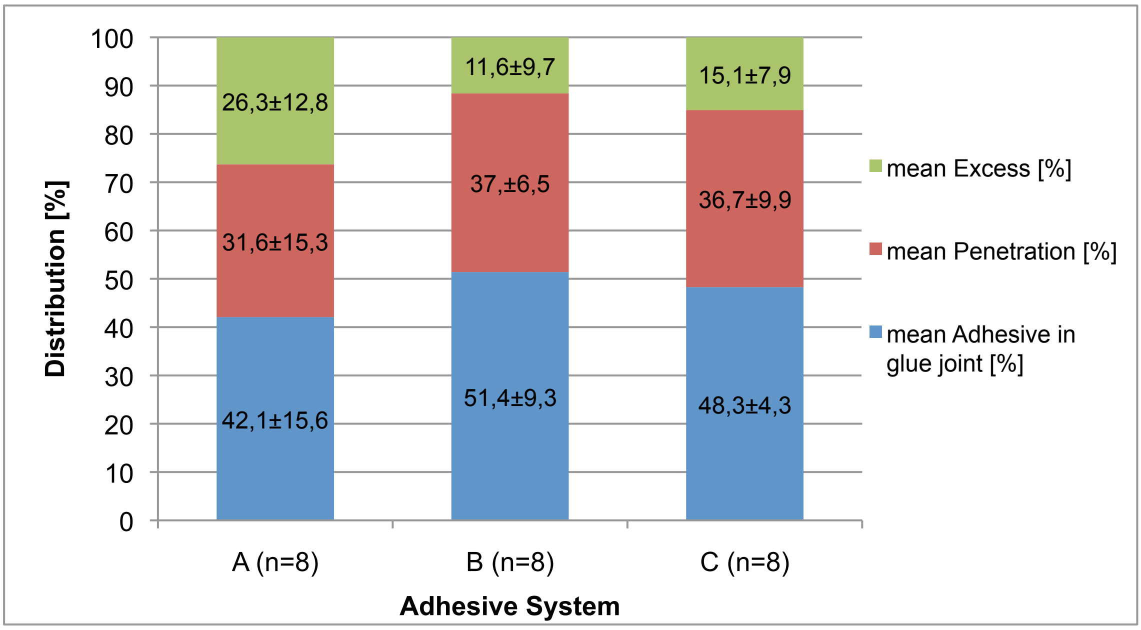

Fig. 26: Mean values plus standard deviation of adhesive distribution of the different adhesive systems: (A) urea-formaldehyde, (B) urea-formaldehyde + nanocellulose, (C) urea-formaldehyde + additive II. (n) sample-size.

As already mentioned in the introduction to this method, it is very important that all individual process steps are made by the same person due to the highly subjective influence of the person conducting the research. Nevertheless, it was decided in this case to combine the results of two different people to achieve a larger sample size. The additionally used results were from a scholar at Wood K plus, who did some preliminary tests with the same samples used for this study. The facts that legitimated the pooling of the results were that firstly this researcher trained the author the procedure of the complete method and the author asked for his advice in difficult and unclear decisions. Secondly, that due to the pooling of the results the standard deviation could be reduced slightly. In table 2 the results before and after pooling the samples are shown. This table shows that the standard deviation could be reduced for every single mean result (except mean adhesive in glue joint for system C) and most importantly, the reduction was highest where also the standard deviation was highest (A).

Table 2: Comparison of results and standard deviation before pooling (n=8) and after pooling (n=12).

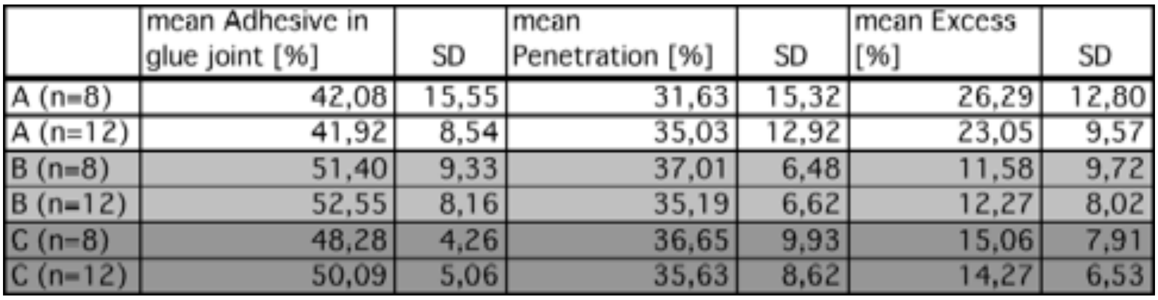

	mean Adhesive in glue joint [%]	SD	mean Penetration [%]	SD	mean Excess [%]	SD
A (n=8)	42,08	15,55	31,63	15,32	26,29	12,80
A (n=12)	41,92	8,54	35,03	12,92	23,05	9,57
B (n=8)	51,40	9,33	37,01	6,48	11,58	9,72
B (n=12)	52,55	8,16	35,19	6,62	12,27	8,02
C (n=8)	48,28	4,26	36,65	9,93	15,06	7,91
C (n=12)	50,09	5,06	35,63	8,62	14,27	6,53

Abbreviations: **A** urea-formaldehyde, **B** urea formaldehyde plus nanocellulose, **C** urea-formaldehyde plus additive 2, **n** sample size, **SD** standard deviation.

In figure 27 the results of table 2 after pooling are graphically displayed. These results were finally used for the statistical analysis. The three different portions of adhesive: adhesive in the glue joint, penetrated adhesive and excess should be tested with a one-way analysis of variance (ANOVA) if there is a statistically significant difference due to the adhesive system. The ANOVA requires normally distributed data and homogeneity in variance of the data.

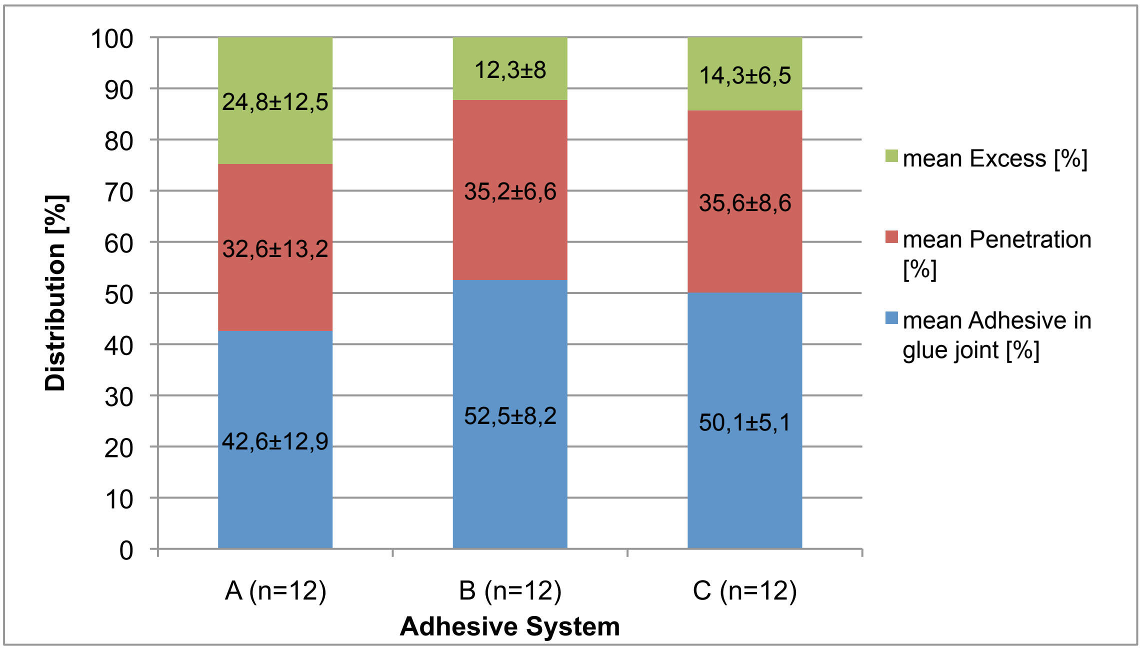

Fig. 27: Mean values plus standard deviation of adhesive distribution of the different adhesive systems after pooling the results: (A) urea-formaldehyde, (B)

urea-formaldehyde + nanocellulose, (C) urea-formaldehyde + additive II. (n) sample-size.

All of these tests were conducted in SPSS. The requirement of normally distributed data was met by all three portions, but homogeneity in variance was not met by the data adhesive in glue joint. A remedial measure to this is the so-called Kruskal-Wallis test, which is immune to heterogeneous variances. With the Kruskal-Wallis test no statistically significant differences in the relative amount of adhesive in the glue joint could be found. This was quite surprising especially for the systems A and B, were the relative difference in the mean values is 9.9%. But at the same time both systems have a high standard deviation. For the penetration of adhesive, where the portion for all three adhesive systems are around 35%, no significant differences were expected and this assumption was proven by the one-way ANOVA. For the excess portion on the other hand, the one-way ANOVA revealed a significant difference due to the adhesive system. With a post-hoc Scheffé-test significant differences were found between the systems A and B as well as A and C, but not between B and C. This means that both adhesive systems with additives have statistically significant less excessive adhesive than the reference system with only urea-formaldehyde. Statistically less excessive adhesive also means on the other hand that there is more adhesive available for bonding, either in the glue joint or penetrated. According to Stehr and Johansson (2000) penetration of adhesive is a necessity for a proper bonding to compensate the mechanical weak boundary layer and anchor to undamaged wood material. Furthermore Gindl et al. (2005) could prove that penetration of resin increases the stiffness of the wood-adhesive interface. The results of this study also mean that the initially stated hypothesis of less penetration of adhesive due to additives can not be proven statistically. Nevertheless a few assumptions underlining this hypothesis can be made based on the results of figure 27 beside statistical significance. Although there is more adhesive in the glue joint in the systems with additives, namely 9.9% for system B and 7.5% for system C, the penetration is just 2.6% and 3.0% more, respectively. In other words, for each percent of adhesive in the glue joint in system A 0.77% of adhesive were penetrated into the particle, compared to 0.67% for system B and 0.71 % for system C. This could be an indication that the additives slightly reduce the penetration of adhesive from the glue joint into the wood particle. A higher sample size in a follow up study would be necessary to prove this theory. A second assumption that can be made based on these results is that a more stable and reproducible distribution of the adhesive can be achieved with additives since the standard deviation is lower for systems with additives in all portions. A more detailed view not on the distribution of the adhesive but on the size of adhesive particles is made in the next two figures. Figure 28 shows the distribution of the quantity of particles sizes. Thus the particles sizes were divided in categories with 25, 100, 250, 1000 and 10000 µm^2. For this analysis only results generated in this work were used due to the fact that the number of adhesive particles of the Wood K plus work is more than double, although the sample size was just half.

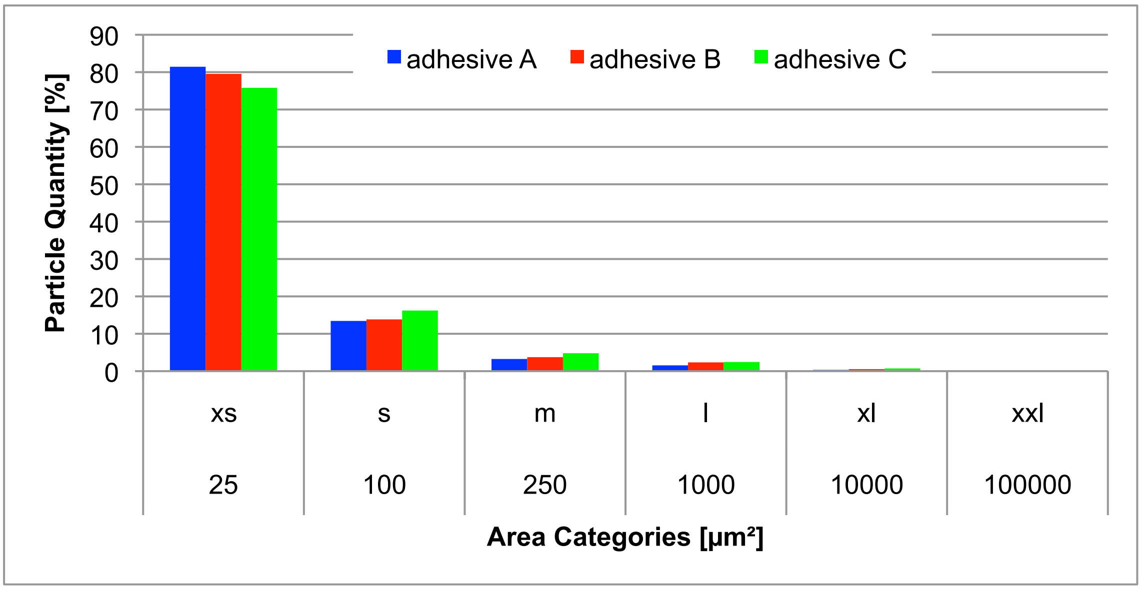

Fig. 28: Distribution of the particle sizes in the different adhesive systems: (A) urea-formaldehyde, (B) urea-formaldehyde + nanocellulose, (C) urea-formaldehyde + additive II.

In this evaluation 9,655 particles for system A, 12,134 for B and 12,012 for C were analyzed. Statistical assessment with the Chi^2-test shows that the zero hypothesis, which states that the particles size distribution is independent of the adhesive system, can be rejected with 1% level of significance.

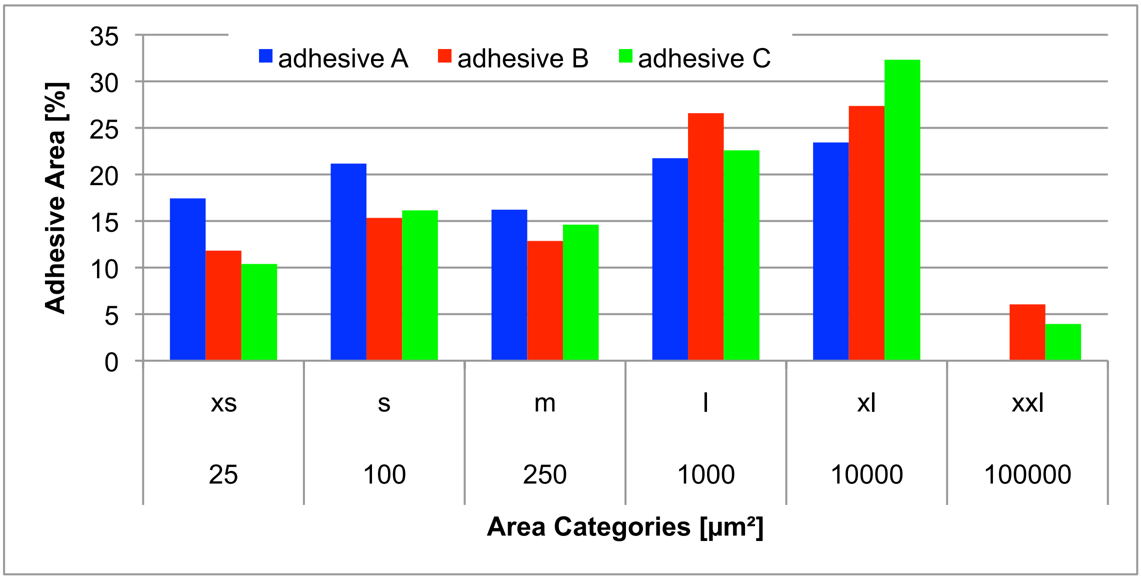

Fig. 29: Percentaged distribution of the adhesive area of different adhesive systems based on particle size: (A) urea-formaldehyde, (B) urea-formaldheyde + nanocellulose, (C) urea-formaldheyde + additive II.

This means that the particle size distribution is highly significant dependent on the adhesive system. The reference adhesive system A has the highest portion of particles smaller than 25 µm^2 followed by system B and C. The bigger the particles get, the smaller is the portion of system A compared to the reinforced systems B and C. This shows that the reinforced systems tend to create bigger adhesive particles or conglomerates than the unreinforced. This assumption is underlined by the results of figure 29, where the percentual distribution of the adhesive area based on the particle size is graphically pictured. It shows that e.g. for system C 32.3% of the adhesive area is made of particles bigger than 1,000 and smaller than 100,000 µm^2, compared to only 23.4% of system B. If these two figures are combined, it can be said that e.g. for system C 32.3% of the adhesive area is made up of 0.72% of all particles with a size of more than 1,000 and smaller than 100,000 µm^2. The reason for this different particle size distribution can just be assumed. First assumption is that the reason lies already in the gluing process. Maybe the adding of the additives immediately after the adding of the glue keeps the glue from distributing properly. Another explanation is that the 1 cm^3 big clusters of additives do not disintegrate completely, hence small conglomerates of nanocellulose remain and bind adhesive.

Some scholars (Eichhorn et al. 2010; Veigel et al. 2011; Veigel et al. 2012) state that additives like nanocellulose lead to a decrease in brittleness and an increase in ductility of the urea-formaldehyde resin and this leads to higher mechanical properties in turn. This increase in ductility could no only be accounted for higher internal bond but may already have an impact during pressing the particle boards in discontinuous laboratory presses. Both reasons that are responsible for pre-curing while pressing according to Dunky and Niemz (2002) can be found in the production of particle boards with a laboratory press: long required waiting times in the open press and a long press-closing time. This means that during the pressing process some adhesive particles are already completely cured (pre-curing) before the compression process is finished. Hence the assumption that due to the high brittleness of urea-formaldehyde these already cured adhesive particles disrupt into smaller particles during the compression process. While on the other hand the reinforcing additives prevent the cured particles in the reinforced adhesive system from disrupting. This theory explains the higher amount of really small particles (< 25 μm^2) in the unreinforced system and the higher quantity of bigger particles in the reinforced systems. Furthermore it also explains the significant higher amount of excessive adhesive in the reference samples.

5 Conclusion

The method of adhesive detection is a novel method in the analysis of adhesive distributions without any publications so far. The advantage of the information about the distribution of the adhesive faces two main disadvantages, the high expenditure of time and the strong subjective influence of the scholar. Due to the time consuming work it was only possible to analyze specimens per adhesive system, in total 24. If further studies with a higher sample size are required, it will be necessary to counteract this drawback by automating and speeding up some process steps. The first process step with high time consumption that could be automated is the microscopy. Furthermore, nearly all process steps after retracing the particles can also be automated by creating specified sequence patterns in Photoshop and imageJ. All the remaining steps in image editing can not be automated and therefore underlie the subjective influence of the scholar e.g. retracing particles. This leads us to the question to what extent it is possible to compare two studies by different authors.

The hypothesis this master thesis is based on, that there is less penetration due to additives, could not be proven statistically. The results show a higher (not significant) amount of adhesive in the bondline and statistically significant less excess for the reinforced adhesive systems compared to the reference. On the other hand a relatively lower penetration rate from the bondline into the wood matter could be observed. This master thesis focused on the absolute amount of penetration, but maybe the penetration rate should be given more attention in a follow-up study. A highly positive effect of the additive system is that overall a higher amount of adhesive is available for bonding either in the bondline or penetrated from the bondline to the wood matter. This could be one explanation for the higher internal bond strength of the adhesive systems B and C. Furthermore it is statistically proved that the addition of additives influences the adhesive particle size. The reference system shows a higher amount of smaller particles compared to the reinforced systems. Combining these results with the result of less excess, the assumption can be drawn that the addition of additives has a positive influence on the resin during the board production process or specimen preparation process.

As already shown in the results of figure 22 to 24, the individual samples show a high variance within the adhesive system and therefore a high standard deviation. Because of this, a follow-up study with a higher size of samples and the above described rationalization of the workflow should be done.

(Veigel et al. 2011)

6 References

Dunky M (1998) Urea–formaldehyde (UF) adhesive resins for wood. International Journal of Adhesion and Adhesives 18:95-107 doi:http://dx.doi.org/10.1016/S0143-7496(97)00054-7

Dunky M, Niemz P (2002) Holzwerkstoffe und Leime. Springer-Verlag, Berlin Heidelberg

Eichhorn SJ et al. (2010) Review: current international research into cellulose nanofibres and nanocomposites. Journal of Materials Science 45:1-33 doi:10.1007/s10853-009-3874-0

Gagliano JM, Frazier CE (2001) Improvements in the fracture cleavage testing of adhesively-bonded wood. Wood and Fiber Science 33:377-385

Gindl W, Sretenovic A, Vincenti A, Müller U (2005) Direct measurement of strain distribution along a wood bond line. Part 2: Effects of adhesive penetration on strain distribution. Holzforschung 59:307 doi:10.1515/HF.2005.051

Habenicht G (2008) Kleben: Grundlagen, Technologien, Anwendungen. Springer, Berlin Heidelberg

López-Suevos F, Eyholzer C, Bordeanu N, Richter K (2010) DMA analysis and wood bonding of PVAc latex reinforced with cellulose nanofibrils. Cellulose 17:387-398 doi:10.1007/s10570-010-9396-8

Müller U, Sretenovic A, Vincenti A, Gindl W (2005) Direct measurement of strain distribution along a wood bond line. Part 1: Shear strain concentration in a lap joint specimen by means of electronic speckle pattern interferometry. Holzforschung 59:300 doi:10.1515/HF.2005.050

Riegler M, Gindl-Altmutter W, Hauptmann M, Müller U (2012) Detection of UF resin on wood particles and in particleboards: potential of selected methods for practice-oriented offline detection. European Journal of Wood and Wood Products 70:829-837 doi:10.1007/s00107-012-0628-5

Standardization ECf (1993) EN 319: Particleboards and fibreboards; determination of tensile strength perpendicular to the plane of the board. Brussels, Belgium

Standardization ECf (2003) EN 312 Spanplatten - Anforderungen.

Standardization ECf (2004) EN 302 Adhesives for load-bearing timber structures - Test methods - Part 1: Determination of longitudinal tensile shear strength.

Stehr M, Johansson I (2000) Weak boundary layers on wood surfaces. Journal of Adhesion Science and Technology 14:1211-1224 doi:10.1163/156856100742168

Thoemen H, Irle M, Sernek M (2010) Wood-Based Panels: An Introduction for Specialists. Brunel University Press

UNECE, FAO (2013) Forest Products - Annual Market Review 2012-2013. Geneva

Van Herwijnen E, Mahrdt EA, Gindl-Altmutter W, Kantner W, Moser J, Müller U, Stöckl F Novel methods to investigate the UF resin distribution within industrial MDF and particleboards. In: International Conference on Wood Adhesives 2013, Toronto, 2013. Forest products society, pp 243-250

Veigel S, Müller U, Keckes J, Obersriebnig M, Gindl-Altmutter W (2011) Cellulose nanofibrils as filler for adhesives: effect on specific fracture energy of solid wood-adhesive bonds. Cellulose 18:1227-1237 doi:10.1007/s10570-011-9576-1

Veigel S, Rathke J, Weigl M, Gindl-Altmutter W (2012) Particle Board and Oriented Strand Board Prepared with Nanocellulose-Reinforced. Adhesive Journal of Nanomaterials 2012:8 doi:10.1155/2012/158503

7 Figures

8 Appendix

Statistics for preliminary work

Density - test normal distribution

Kolmogorov-Smirnov-Anpassungstest

	Density
N	26

Parameter der Normalverteilung[a,b]	Mittelwert	652,8077
	Standardabweichung	33,09987
Extremste Differenzen	Absolut	,148
	Positiv	,148
	Negativ	-,101
Kolmogorov-Smirnov-Z		,756
Asymptotische Signifikanz (2-seitig)		,617

a. Die zu testende Verteilung ist eine Normalverteilung.

b. Aus den Daten berechnet.

```
DATASET ACTIVATE DatenSet1.

ONEWAY Density BY System
  /STATISTICS DESCRIPTIVES HOMOGENEITY
  /MISSING ANALYSIS
  /POSTHOC=SCHEFFE ALPHA(0.05).
```

Density - comparison of means

ONEWAY deskriptive Statistiken

Density

	N	Mittelwert	Standardabweichung	Standardfehler	95%-Konfidenzintervall für den Mittelwert		Minimum	Maximum
					Untergrenze	Obergrenze		
A	10	635,6000	23,52398	7,43894	618,7720	652,4280	592,00	670,00
B	6	648,5000	23,34738	9,53153	623,9984	673,0016	625,00	678,00
C	10	672,6000	37,55648	11,87640	645,7337	699,4663	617,00	717,00
Gesamt	26	652,8077	33,09987	6,49142	639,4384	666,1770	592,00	717,00

Test der Homogenität der Varianzen

Density

Levene-Statistik	df1	df2	Signifikanz
3,482	2	23	,048

Einfaktorielle ANOVA

Density

	Quadratsumme	df	Mittel der Quadrate	F	Signifikanz
Zwischen den Gruppen	6989,738	2	3494,869	3,940	,034
Innerhalb der Gruppen	20400,300	23	886,970		
Gesamt	27390,038	25			

Post-Hoc-Tests

Mehrfachvergleiche

Abhängige Variable: Density

Scheffé-Prozedur

(I) System	(J) System	Mittlere Differenz (I-J)	Standardfehler	Signifikanz	95%-Konfidenzintervall	
					Untergrenze	Obergrenze
A	B	-12,90000	15,37938	,707	-53,1348	27,3348
	C	-37,00000*	13,31893	,036	-71,8444	-2,1556
B	A	12,90000	15,37938	,707	-27,3348	53,1348
	C	-24,10000	15,37938	,311	-64,3348	16,1348
C	A	37,00000*	13,31893	,036	2,1556	71,8444

B	24,10000	15,37938	,311	-16,1348	64,3348

*. Die Differenz der Mittelwerte ist auf dem Niveau 0.05 signifikant.

Homogene Untergruppen

Density

Scheffé-Prozedur[a,b]

System	N	Untergruppe für Alpha = 0.05.
		1
A	10	635,6000
B	6	648,5000
C	10	672,6000
Signifikanz		,061

Die Mittelwerte für die in homogenen Untergruppen befindlichen Gruppen werden angezeigt.

a. Verwendet ein harmonisches Mittel für Stichprobengröße = 8,182.

b. Die Gruppengrößen sind nicht identisch. Es wird das harmonische Mittel der Gruppengrößen verwendet. Fehlerniveaus des Typs I sind nicht garantiert.

Density - comparison of means

Kruskal-Wallis-Test

Ränge

	System	N	Mittlerer Rang
Density	A	10	9,85
	B	6	13,33
	C	10	17,25
	Gesamt	26	

Statistik für Test[a,b]

	Density
Chi-Quadrat	4,687
df	2
Asymptotische Signifikanz	,096

a. Kruskal-Wallis-Test

b. Gruppenvariable: System

```
ONEWAY Density BY System
  /STATISTICS DESCRIPTIVES HOMOGENEITY
  /MISSING ANALYSIS
  /POSTHOC=SCHEFFE GH ALPHA(0.05).
```

Internal bond strength - test normal distribution

Kolmogorov-Smirnov-Anpassungstest

	IB_density_corr

N		26
Parameter der Normalverteilung[a,b]	Mittelwert	,5908
	Standardabweichung	,13290
Extremste Differenzen	Absolut	,116
	Positiv	,089
	Negativ	-,116
Kolmogorov-Smirnov-Z		,592
Asymptotische Signifikanz (2-seitig)		,875

a. Die zu testende Verteilung ist eine Normalverteilung.

b. Aus den Daten berechnet.

```
ONEWAY IB_density_corr BY System
  /STATISTICS DESCRIPTIVES HOMOGENEITY
  /MISSING ANALYSIS
  /POSTHOC=SCHEFFE GH ALPHA(0.05).
```

Internal bond strength - comparison of means

ONEWAY deskriptive Statistiken

IB_density_corr

	N	Mittelwert	Standardabweichung	Standardfehler	95%-Konfidenzintervall für den Mittelwert		Minimum	Maximum
					Untergrenze	Obergrenze		
A	10	,4640	,10013	,03166	,3924	,5356	,32	,66
B	6	,6267	,06377	,02603	,5597	,6936	,54	,72
C	10	,6960	,07589	,02400	,6417	,7503	,54	,77
Gesamt	26	,5908	,13290	,02606	,5371	,6445	,32	,77

Test der Homogenität der Varianzen

IB_density_corr

Levene-Statistik	df1	df2	Signifikanz
,367	2	23	,697

Einfaktorielle ANOVA

IB_density_corr

	Quadratsumme	df	Mittel der Quadrate	F	Signifikanz
Zwischen den Gruppen	,279	2	,140	19,767	,000
Innerhalb der Gruppen	,162	23	,007		
Gesamt	,442	25			

Post-Hoc-Tests

Mehrfachvergleiche

Abhängige Variable: IB_density_corr

	(I) System	(J) System	Mittlere Differenz (I-J)	Standardfehler	Signifikanz	95%-Konfidenzintervall	
						Untergrenze	Obergrenze
Scheffé-Prozedur	A	B	-,16267*	,04339	,004	-,2762	-,0491
		C	-,23200*	,03758	,000	-,3303	-,1337
	B	A	,16267*	,04339	,004	,0491	,2762
		C	-,06933	,04339	,298	-,1829	,0442

	C	A	,23200*	,03758	,000	,1337	,3303
		B	,06933	,04339	,298	-,0442	,1829
Games-Howell	A	B	-,16267*	,04099	,004	-,2701	-,0553
		C	-,23200*	,03973	,000	-,3341	-,1299
	B	A	,16267*	,04099	,004	,0553	,2701
		C	-,06933	,03541	,165	-,1636	,0249
	C	A	,23200*	,03973	,000	,1299	,3341
		B	,06933	,03541	,165	-,0249	,1636

*. Die Differenz der Mittelwerte ist auf dem Niveau 0.05 signifikant.

Homogene Untergruppen

IB_density_corr

	System	N	Untergruppe für Alpha = 0.05.	
			1	2
Scheffé-Prozedur[a,b]	A	10	,4640	
	B	6		,6267
	C	10		,6960
	Signifikanz		1,000	,269

Die Mittelwerte für die in homogenen Untergruppen befindlichen Gruppen werden angezeigt.

a. Verwendet ein harmonisches Mittel für Stichprobengröße = 8,182.

b. Die Gruppengrößen sind nicht identisch. Es wird das harmonische Mittel der Gruppengrößen verwendet. Fehlerniveaus des Typs I sind nicht garantiert.

Statistics for distribution of adhesive in particle boards

Test normal distribution

Tests auf Normalverteilung

	System	Kolmogorov-Smirnov[a]			Shapiro-Wilk		
		Statistik	df	Signifikanz	Statistik	df	Signifikanz
Adhesiveingluejoint	A	,155	12	,200*	,965	12	,850
	B	,195	12	,200*	,918	12	,270
	C	,155	12	,200*	,927	12	,352
Penetration	A	,158	12	,200*	,963	12	,824
	B	,158	12	,200*	,938	12	,471
	C	,185	12	,200*	,929	12	,371
Excess	A	,147	12	,200*	,951	12	,653
	B	,178	12	,200*	,899	12	,153
	C	,194	12	,200*	,904	12	,177

*. Dies ist eine untere Grenze der echten Signifikanz.

a. Signifikanzkorrektur nach Lilliefors

```
ONEWAY Adhesiveingluejoint Penetration Excess BY System
  /STATISTICS DESCRIPTIVES HOMOGENEITY
  /MISSING ANALYSIS
  /POSTHOC=SCHEFFE BONFERRONI T3 ALPHA(0.05).
```

Comparison of means

ONEWAY deskriptive Statistiken

	N	Mittelwert	Standardabweichung	Standardfehler	95%-Konfidenzintervall für den Mittelwert	Minimum	Maximum

						Untergrenze	Obergrenze		
Adhesiveingluejoint	A	12	42,5816	12,90632	3,72573	34,3813	50,7818	21,92	69,88
	B	12	52,5464	8,16088	2,35584	47,3613	57,7316	40,01	63,79
	C	12	50,0905	5,05723	1,45990	46,8773	53,3037	43,14	57,50
	Gesamt	36	48,4062	9,99013	1,66502	45,0260	51,7863	21,92	69,88
Penetration	A	12	32,6367	13,15064	3,79626	24,2811	40,9922	12,00	53,95
	B	12	35,1867	6,61683	1,91011	30,9825	39,3908	26,57	46,22
	C	12	35,6350	8,62075	2,48860	30,1576	41,1124	21,08	48,39
	Gesamt	36	34,4861	9,65727	1,60955	31,2186	37,7537	12,00	53,95
Excess	A	12	24,7808	12,45876	3,59653	16,8649	32,6967	8,01	52,20
	B	12	12,2642	8,01656	2,31418	7,1707	17,3576	1,30	32,35
	C	12	14,2733	6,53493	1,88647	10,1212	18,4254	6,09	27,92
	Gesamt	36	17,1061	10,64834	1,77472	13,5032	20,7090	1,30	52,20

Test der Homogenität der Varianzen

	Levene-Statistik	df1	df2	Signifikanz
Adhesiveingluejoint	4,590	2	33	,017
Penetration	3,263	2	33	,051
Excess	1,912	2	33	,164

Einfaktorielle ANOVA

	Quadratsumme	df	Mittel der Quadrate	F	Signifikanz

Adhesiveingluejoint	Zwischen den Gruppen	646,859	2	323,430	3,750	,034
	Innerhalb der Gruppen	2846,236	33	86,250		
	Gesamt	3493,096	35			
Penetration	Zwischen den Gruppen	62,774	2	31,387	,324	,726
	Innerhalb der Gruppen	3201,429	33	97,013		
	Gesamt	3264,203	35			
Excess	Zwischen den Gruppen	1084,445	2	542,223	6,204	,005
	Innerhalb der Gruppen	2884,103	33	87,397		
	Gesamt	3968,548	35			

Post-Hoc-Tests

Mehrfachvergleiche

Abhängige Variable		(I) System	(J) System	Mittlere Differenz (I-J)	Standardfehler	Signifikanz	95%-Konfidenzintervall	
							Untergrenze	Obergrenze
Adhesiveingluejoint	Scheffé-Prozedur	A	B	-9,96488*	3,79143	,043	-19,6830	-,2468
			C	-7,50896	3,79143	,157	-17,2270	2,2091
		B	A	9,96488*	3,79143	,043	,2468	19,6830
			C	2,45592	3,79143	,812	-7,2622	12,1740
		C	A	7,50896	3,79143	,157	-2,2091	17,2270
			B	-2,45592	3,79143	,812	-12,1740	7,2622
	Bonferroni	A	B	-9,96488*	3,79143	,039	-19,5277	-,4021

			C	-7,50896	3,79143	,168	-17,0718	2,0538
		B	A	9,96488*	3,79143	,039	,4021	19,5277
			C	2,45592	3,79143	1,000	-7,1069	12,0187
		C	A	7,50896	3,79143	,168	-2,0538	17,0718
			B	-2,45592	3,79143	1,000	-12,0187	7,1069
	Dunnett-T3	A	B	-9,96488	4,40807	,101	-21,4742	1,5445
			C	-7,50896	4,00155	,215	-18,2495	3,2316
		B	A	9,96488	4,40807	,101	-1,5445	21,4742
			C	2,45592	2,77152	,758	-4,7884	9,7003
		C	A	7,50896	4,00155	,215	-3,2316	18,2495
			B	-2,45592	2,77152	,758	-9,7003	4,7884
Penetration	Scheffé-Prozedur	A	B	-2,55000	4,02105	,819	-12,8566	7,7566
			C	-2,99833	4,02105	,759	-13,3050	7,3083
		B	A	2,55000	4,02105	,819	-7,7566	12,8566
			C	-,44833	4,02105	,994	-10,7550	9,8583
		C	A	2,99833	4,02105	,759	-7,3083	13,3050
			B	,44833	4,02105	,994	-9,8583	10,7550
	Bonferroni	A	B	-2,55000	4,02105	1,000	-12,6919	7,5919
			C	-2,99833	4,02105	1,000	-13,1403	7,1436
		B	A	2,55000	4,02105	1,000	-7,5919	12,6919
			C	-,44833	4,02105	1,000	-10,5903	9,6936
		C	A	2,99833	4,02105	1,000	-7,1436	13,1403
			B	,44833	4,02105	1,000	-9,6936	10,5903
	Dunnett-T3	A	B	-2,55000	4,24972	,907	-13,7945	8,6945
			C	-2,99833	4,53924	,880	-14,8275	8,8309
		B	A	2,55000	4,24972	,907	-8,6945	13,7945

Excess			C	-,44833	3,13714	,998	-8,5657	7,6691
		C	A	2,99833	4,53924	,880	-8,8309	14,8275
			B	,44833	3,13714	,998	-7,6691	8,5657
	Scheffé-Prozedur	A	B	12,51667*	3,81657	,010	2,7342	22,2992
			C	10,50750*	3,81657	,033	,7250	20,2900
		B	A	-12,51667*	3,81657	,010	-22,2992	-2,7342
			C	-2,00917	3,81657	,871	-11,7917	7,7733
		C	A	-10,50750*	3,81657	,033	-20,2900	-,7250
			B	2,00917	3,81657	,871	-7,7733	11,7917
	Bonferroni	A	B	12,51667*	3,81657	,007	2,8905	22,1429
			C	10,50750*	3,81657	,029	,8813	20,1337
		B	A	-12,51667*	3,81657	,007	-22,1429	-2,8905
			C	-2,00917	3,81657	1,000	-11,6354	7,6170
		C	A	-10,50750*	3,81657	,029	-20,1337	-,8813
			B	2,00917	3,81657	1,000	-7,6170	11,6354
	Dunnett-T3	A	B	12,51667*	4,27674	,025	1,3606	23,6727
			C	10,50750	4,06126	,056	-,2116	21,2266
		B	A	-12,51667*	4,27674	,025	-23,6727	-1,3606
			C	-2,00917	2,98567	,875	-9,7190	5,7007
		C	A	-10,50750	4,06126	,056	-21,2266	,2116
			B	2,00917	2,98567	,875	-5,7007	9,7190

*. Die Differenz der Mittelwerte ist auf dem Niveau 0.05 signifikant.

Homogene Untergruppen

Adhesiveingluejoint

	System	N	Untergruppe für Alpha = 0.05.	
			1	2
Scheffé-Prozedur[a]	A	12	42,5816	
	C	12	50,0905	50,0905
	B	12		52,5464
	Signifikanz		,157	,812

Die Mittelwerte für die in homogenen Untergruppen befindlichen Gruppen werden angezeigt.

a. Verwendet ein harmonisches Mittel für Stichprobengröße = 12,000.

Penetration

	System	N	Untergruppe für Alpha = 0.05.
			1
Scheffé-Prozedur[a]	A	12	32,6367
	B	12	35,1867
	C	12	35,6350
	Signifikanz		,759

Die Mittelwerte für die in homogenen Untergruppen befindlichen Gruppen werden angezeigt.

a. Verwendet ein harmonisches Mittel für Stichprobengröße = 12,000.

Excess

	System	N	Untergruppe für Alpha = 0.05.	
			1	2
Scheffé-Prozedur[a]	B	12	12,2642	
	C	12	14,2733	
	A	12		24,7808
	Signifikanz		,871	1,000

Die Mittelwerte für die in homogenen Untergruppen befindlichen Gruppen werden angezeigt.

a. Verwendet ein harmonisches Mittel für Stichprobengröße = 12,000.

Nichtparametrische Tests

Kruskal-Wallis-Test

Ränge

	System	N	Mittlerer Rang
Adhesiveingluejoint	A	12	12,67
	B	12	22,42
	C	12	20,42
	Gesamt	36	

Statistik für Test^{a,b}

	Adhesiveingluejoint
Chi-Quadrat	5,734
df	2
Asymptotische Signifikanz	,057

a. Kruskal-Wallis-Test

b. Gruppenvariable: System

Chi^2-Test – Distribution of particle size

beobachtete Werte:

0		Leim A	Leim B	Leim C	Summe:
25	xs	7863	9650	9106	26619
100	s	1297	1680	1948	4925
250	m	314	454	575	1343
1000	l	149	284	294	727
100000	xl	32	66	89	187
	Summe:	9655	12134	12012	33801

erwartete Werte:

0		Leim A	Leim B	Leim C
25	xs	7603,52	9555,78	9459,70
100	s	1406,79	1767,99	1750,22
250	m	383,62	482,11	477,27
1000	l	207,66	260,98	258,36
10000	xl	53,42	67,13	66,45

Für den Chi-Quadrat-Test wurden die Klasse 10000 u. 100000 zusammengelegt, da sonst die Bedingung - erwartete Werte immer >=5 - nicht erfüllt worden wäre.

empirische chi2-Werte

Leim A	Leim B	Leim C
8,86	0,93	13,23
8,57	4,38	22,35
12,63	1,64	20,01
16,57	2,03	4,92
8,59	0,02	7,65

Summe emp. chi2 Werte: 132,37

kritischer chi2 Wert mit 8 >

Freiheitsgraden und (1-α)=0,99: 20,09

Die Nullhypthese, dass die Größenverteilung unabhängig vom Leimsystem ist, wird mit einer Irrtumswahrscheinlichkeit von 1 % abgelehnt